Southern Blot Analysis

DNA was extracted from cardiac tissues, and a Southern blot analysis was performed to measure the mtDNA copy number as described earlier.[9] Primers for the mtDNA probe corresponded to nucleotides 2424 to 3605 of the mouse mitochondrial genome, and those for the nuclear-encoded mouse 18S rRNA probe corresponded to nucleotides 435 to 1951 of the human 18S rRNA genome. The mtDNA levels were normalized to the abundance of the 18S rRNA gene run on the same gel.

RNA Isolation and Northern Blot Analysis

Total RNA was isolated from frozen LV by the guanidinium method, and a Northern hybridization analysis was performed according to methods described previously.[9] Probes for mtRNA analysis were prepared by amplification of nucleotides 1209 to 2606 (probe 1), nucleotides 3351 to 7570 (probe 2), nucleotides 8861 to 14549 (probe 3), and nucleotides 14729 to 15837 (probe 4) of mtDNA from mouse genomic DNA.

Mitochondrial Enzyme Activity

The specific activity of complex I, complex II, complex III, and complex IV was measured in the myocardial tissues according to methods described previously.[9] The specific enzymatic activity of rotenone-sensitive NADH-ubiquinone oxidoreductase (complex I) was measured by a reduction of the ubiquinone analogue decylubiquinone. For the activity of succinate-ubiquinone oxidoreductase (complex II), the reduction of 2,6-dichlorophenolindophenol, when coupled to complex II–catalyzed reduction of decylubiquinone, was measured. For the specific activity of ubiquinol/cytochrome *c* oxidoreductase (complex III), the reduction of cytochrome *c* catalyzed by complex III in the presence of reduced decylubiquinone was monitored. The specific activity of cytochrome *c* oxidase (complex IV) was measured by following the oxidation of reduced cytochrome *c*, which had been prepared in the presence of dithionite. All enzymatic activities were expressed as nanomoles per minute per milligram protein.

Echocardiographic and Hemodynamic Measurements

After 4 weeks of surgery, echocardiographic studies were performed under light anesthesia with tribromoethanol/amylene hydrate (Avertin; 2.5% wt/vol, 8 μL/g IP) and spontaneous respiration. A 2D parasternal short-axis view of the LV was obtained at the level of the papillary muscles. In general, the best views were obtained with the transducer lightly applied to the mid upper left anterior chest wall. The transducer was then gently moved cephalad or caudad and angulated until desirable images were obtained. After it was ensured that the imaging was on axis (based on roundness of the LV cavity), 2D targeted M-mode tracings were recorded at a paper speed of 50 mm/s. Our previous study has shown that the intraobserver and interobserver variabilities of our echocardiographic measurements for LV dimensions were small, and measurements made in the same animals on separate days were highly reproducible.[17] Then, under the same anesthesia with Avertin, a 1.4F micromanometer-tipped catheter (Millar Instruments) was inserted into the right carotid artery and then advanced into the LV to measure pressures.[17]

Infarct Size

To measure the infarct size after 28 days of MI, the heart was excised, and the LVs were cut from apex to base into 3 transverse sections. Five-micrometer sections were cut and stained with Masson's trichrome. Infarct length was measured along the endocardial and epicardial surfaces from each of the cardiac sections, and the values from all specimens were summed. Infarct size (in percentage) was calculated as total infarct circumference divided by total cardiac circumference.[17]

In addition, to measure infarct size after 24 hours when most animals are still alive, a separate group of animals including WT-MI (n=6) and Tg-MI (n=6) was created. After 24 hours of coronary artery ligation, Evans blue dye (1%) was perfused into the aorta and coronary arteries, and tissue sections were weighed and then incubated with a 1.5% triphenyltetrazolium chloride solution. The infarct area (pale), the area at risk (not blue), and the total LV area from each section were measured.[18] In our preliminary study, we confirmed excellent reliability of infarct size measurements, in which a morphometric methodology similar to that used in this study was used. The intraobserver and interobserver variabilities between 2 measurements divided by these means, expressed as a percentage, were <5%.

Histopathology

After in vivo hemodynamic studies, the heart was excised and dissected into the right and left ventricles, including the septum. Five-micrometer sections were cut and stained with Masson's trichrome. Myocyte cross-sectional area and collagen volume fraction were determined by the quantitative morphometry of LV tissue sections.[17]

For assessment of mitochondrial ultrastructure by electron microscopy, LV tissues were fixed in a mixture of 1% glutaraldehyde and 4% paraformaldehyde in 0.1 mol/L phosphate buffer at pH 7.4 for 2 hours at room temperature. After they were washed in 0.1 mol/L phosphate buffer containing 0.25 mol/L sucrose, they were postfixed with 1% osmium tetroxide for 1 hour at room temperature. The tissues were then block-stained with 1% uranyl acetate in 50% methanol for 2 hours, dehydrated in a graded series of ethanol, and embedded in Epon. Ultrathin sections were double stained with uranyl acetate and lead citrate and then were observed under an electron microscope (Hitachi H7000). For quantitative morphometric analysis, the number and size of the mitochondria were examined according to methods described previously.[9] The number of mitochondria and the cross-sectional area (size) of each mitochondrion were measured within a sampling region of 100 square sarcomeres (sm^2). Eighteen regions were selected at random for each specimen, and for all regions the averages of mitochondrial number and cross-sectional area were calculated.

Apoptosis

To detect apoptosis, LV tissue sections were stained with terminal deoxynucleotidyl transferase–mediated dUTP nick end-labeling (TUNEL) staining. The number of TUNEL-positive cardiac myocyte nuclei was counted, and the data were normalized per 10^5 total nuclei identified by hematoxylin-positive staining in the same sections. We further examined whether apoptosis is present by the more sensitive ligation-mediated PCR fragmentation assays (Maxim Biotech Inc).[18]

Statistical Analysis

Data are expressed as mean±SEM. Survival analysis was performed by the Kaplan-Meier method, and between-group difference in survival was tested by the log-rank test. Between-group comparison of means was performed by 1-way ANOVA, followed by *t* tests. The Bonferroni correction was done for multiple comparisons of means. $P<0.05$ was considered statistically significant.

Results

Characterization of Human TFAM Tg Mice

Human *TFAM* cDNA was used to generate Tg mice (Figure 1A). Four lines of Tg mice were confirmed by PCR. These lines were viable and fertile, and there were no detectable differences in cardiac size and structure between Tg and WT mice either macroscopically or microscopically.

We analyzed TFAM protein levels in various tissues by Western blot analysis using anti-human TFAM antibody. We found a robust expression of human TFAM protein in the heart and skeletal muscle, but it was barely detected in the lung, liver, and kidney (Figure 1B). Among 4 established lines of Tg mice, 1 line that expressed the highest level of the human TFAM protein in the heart was used for further

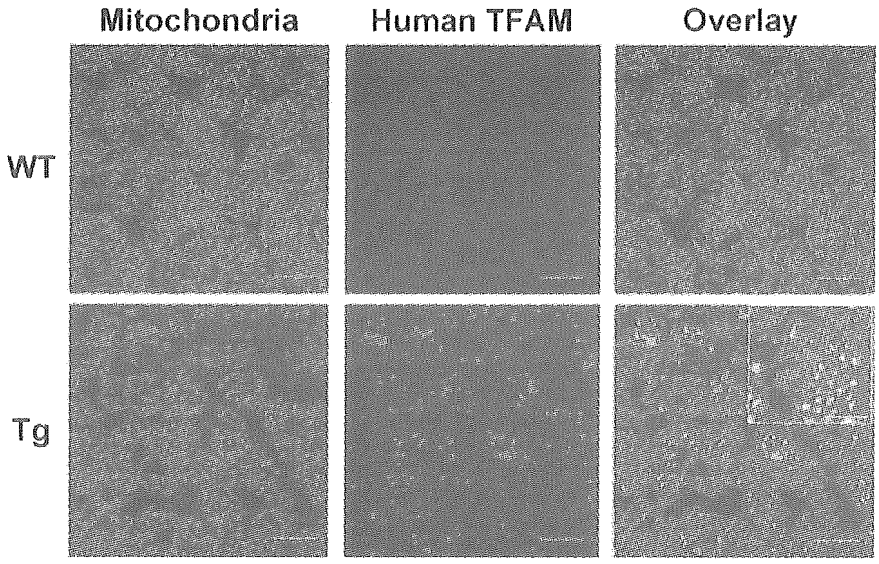

Figure 2. Myocardial tissue sections from WT (top) and Tg (bottom) mice were double-stained with MitoTracker dye (red) and a human TFAM specific antibody (green). Immunoreactivity for human TFAM was observed in the cytoplasm of cardiac myocytes. Merged images show that TFAM was colocalized with the mitochondria (yellow). Bar=20 μm. Inset shows merged images with higher magnification; bar=10 μm.

experiments. The endogenous expression level of the mouse Tfam protein was not modified or downregulated by the overexpression of human *TFAM* gene (Figure 1C). Immunohistochemical studies showed homogeneous human TFAM distribution in cardiac myocytes and colocalized with the mouse mitochondria (Figure 2). Human TFAM staining showed a relatively spotty staining pattern. With higher magnification, its expression appeared not to be restricted to a specific site of mitochondria (Figure 2, inset). These results suggest that the human TFAM exerts an expression pattern similar to that observed for the endogenous mouse Tfam and may function in the mouse heart.

MtDNA Copy Number and Mitochondrial Enzymes

We created MI in male Tg mice (Tg-MI) and nontransgenic wild-type littermates (WT-MI). Sham operation without coronary artery ligation was also performed in WT (WT-sham) and Tg (Tg-sham) mice. After 4 weeks of surgery, we measured mtDNA copy number, expressed as the ratio of mtDNA to nuclear DNA (18S rRNA), in the myocardial tissue by a Southern blot analysis. In parallel to an increase in TFAM protein, mtDNA copy number increased in the heart from Tg animals compared with WT controls (Figure 3A). In WT-MI animals, mtDNA copy number in the noninfarcted LV showed a 41% decrease ($P<0.01$) compared with sham mice, which was significantly prevented and preserved at a normal level in Tg-MI mice (Figure 3A).

To determine the effects of mtDNA copy number alterations on mtRNA, mtRNA transcript levels were measured by Northern blot analysis. As previously reported,[9] mtRNA transcript levels, including ND1+ND2, ND4, ND4L, ND5, cytochrome *b*, COI, COII, and COIII transcripts as well as 16S rRNA, were lower in WT-MI than those in WT-sham. However, overexpression of human *TFAM* did not increase, and even decreased, these mRNA levels in Tg-sham as well as in Tg-MI (online-only Data Supplement I). These results indicate that the regulation of mtRNA transcripts is dissociated from that of mtDNA copy number.

We next measured the respiratory chain enzyme activities. Despite the significant increase in mtDNA copy number in the heart from Tg, complex I, complex II, complex III, and complex IV demonstrated no significant changes in the enzymatic activity in comparison with WT controls (Figure 3B). Consistent with mtDNA copy number, the enzymatic activities of complex I, complex III, and complex IV were significantly lower in the noninfarcted LV from WT-MI than those from WT-sham. Most importantly, there was no such decrease observed in Tg-MI (Figure 3B). The enzymatic activity of complex II, exclusively encoded by nuclear DNA, was not altered in either group. These results indicate that mtDNA and mitochondrial enzymatic activities are downregulated in the hearts after MI, and human *TFAM* gene overexpression efficiently counteracts these mitochondrial deficiencies.

The overall number of mitochondria and the overall average size of the mitochondria demonstrated no significant changes in Tg-sham in comparison with WT controls. In contrast, the mitochondrial number was significantly increased and their size was decreased in WT-MI, both of which were attenuated in Tg-MI (online-only Data Supplement II).

Survival

The survival analysis was performed in 4 groups of mice during the study period of 4 weeks; WT-sham (n=20), WT-MI (n=21), Tg-sham (n=29), and Tg-MI (n=29). There were no deaths in sham-operated groups. The survival rate was significantly higher in Tg-MI compared with WT-MI (100% versus 66%; $P<0.01$; Figure 4A).

Infarct Size

We determined the infarct size by morphometric analysis in the surviving mice 28 days after MI, and it was comparable between WT-MI and Tg-MI (Figure 4B). To further confirm that overexpression of *TFAM* gene did not alter the infarct size, both area at risk and infarct area were measured in a separate group of mice 24 hours after coronary artery ligation.

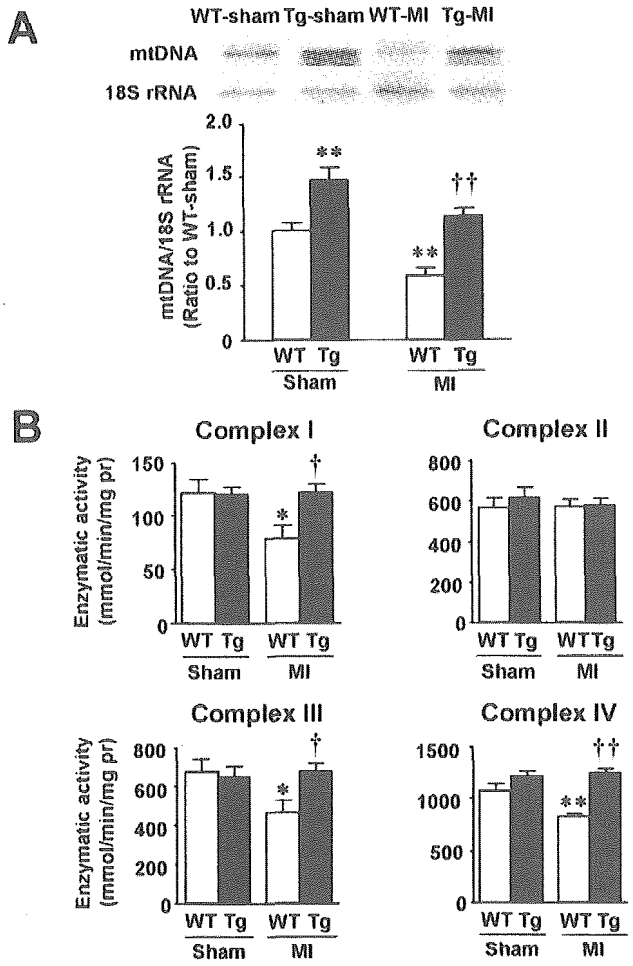

Figure 3. mtDNA and mitochondrial function. A, top, Southern blot analysis of mtDNA copy number in total DNA extracts from the heart from WT-sham, Tg-sham, WT-MI, and Tg-MI mice. Top bands show signals from the mtDNA fragment, and bottom bands show signals from the nuclear DNA fragment containing the 18S rRNA gene. A, bottom, Summary data for a Southern blot analysis of mtDNA copy number in 4 groups of animals (n=8 for each). Data were obtained by a densitometric quantification of the Southern blots such as those shown in A. B, Enzymatic activity of respiratory chain complex I, complex II, complex III, and complex IV in isolated mitochondria from 4 groups of animals (n=6 for each). Each assay was done in triplicate. Values are mean±SEM. *P<0.05, **P<0.01 for difference from WT-sham values. †P<0.05, ††P<0.01 for difference from WT-MI values. pr indicates protein.

The infarct size (infarct/risk area) was also comparable between WT-MI and Tg-MI mice (84.5±0.4% for n=6 versus 83.2±1.1% for n=6; P=NS; Figure 4C).

Cardiac Function and Structure

The echocardiographic studies of surviving mice at 4 weeks showed that cardiac diameters were significantly increased in WT-MI over the values in WT-sham or Tg-sham. Tg-MI showed less cavity dilatation and improved contractile function compared with WT-MI (Figure 5).

There was no significant difference in heart rate and aortic blood pressure among 4 groups of mice (Table). LV end-diastolic pressure increased in WT-MI and was significantly attenuated in Tg-MI. Coinciding with increased LV end-diastolic pressure, lung weight/body weight increased in WT-MI

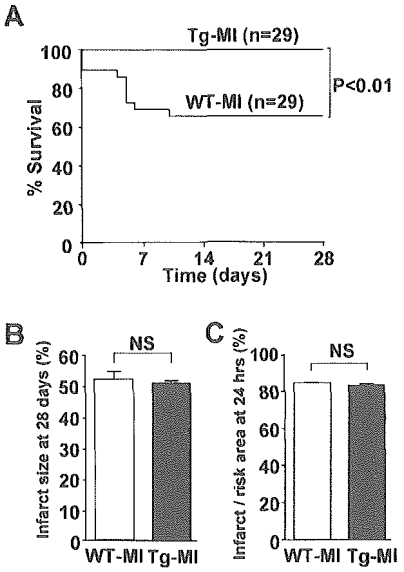

Figure 4. Survival and infarct size. A, Kaplan-Meier survival analysis. Percentages of surviving WT-MI (n=29) and Tg-MI (n=29) mice were plotted. Between-group difference was tested by the log-rank test. B, Infarct size values from WT-MI (n=6) and Tg-MI (n=6) mice in surviving mice 28 days after MI. C, Infarct size (infarct/risk area) values from WT-MI (n=6) and Tg-MI (n=6) mice 24 hours after MI. Values are mean±SEM.

and was also attenuated in Tg-MI (Table). The prevalence of pleural effusion, a clinical sign of heart failure, was significantly lower in Tg-MI than that in WT-MI (Table).

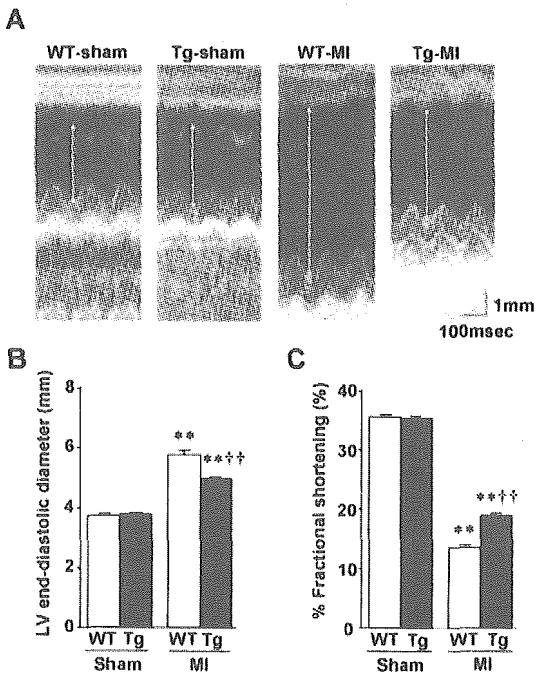

Figure 5. A, Representative M-mode echocardiograms obtained from WT-sham, Tg-sham, WT-MI, and Tg-MI mice. Arrows indicate LV end-diastolic diameter. B, C, Summary data for echocardiographic measurements in 4 groups of animals (n=6 for each). LV end-diastolic diameter (B) and percent fractional shortening (C) are shown. Values are mean±SEM. **P<0.01 for difference from WT-sham values; ††P<0.01 for difference from WT-MI values.

Characteristics of Animal Models

	WT-Sham (n=20)	Tg-Sham (n=21)	WT-MI (n=19)	Tg-MI (n=29)
Hemodynamic data				
Heart rate, bpm	469±6	471±4	479±11	477±4
Mean aortic pressure, mm Hg	77±4	76±2	73±1	74±1
LV EDP, mm Hg	0.7±0.5	0.7±0.4	13.1±2.0**	4.3±0.8*‡
Organ weight data				
Body weight, g	27.3±0.4	26.7±0.4	26.2±0.5	26.0±0.2
LV weight/body weight, mg/g	3.14±0.07	3.23±0.05	3.88±0.24**	3.69±0.09**
RV weight/body weight, mg/g	0.95±0.05	0.98±0.04	1.39±0.12**	1.12±0.05†
Lung weight/body weight, mg/g	5.3±0.1	5.3±0.1	8.3±0.6**	6.4±0.3‡
Pleural effusion, %	0	0	63**	31**†

Values are mean±SEM. EDP indicates end-diastolic pressure; RV, right ventricular.
**$P<0.01$ vs WT-sham; †$P<0.05$, ‡$P<0.01$ vs WT-MI.

Cross-sectional area of cardiac myocytes, an index of cellular hypertrophy, increased in the noninfarcted LV from WT-MI and was significantly attenuated in Tg-MI (Figure 6A). Collagen volume fraction, an index of myocardial interstitial fibrosis, also increased in the noninfarcted LV from WT-MI and was significantly smaller in Tg-MI (Figure 6B). These results indicate that TFAM efficiently counteracts structural and functional deterioration in post-MI hearts.

Apoptosis

To detect apoptosis, myocardial tissue sections were stained with TUNEL staining. TUNEL-positive nuclei were rarely seen in control mice, whereas their number increased in the noninfarcted LV from WT-MI and was significantly decreased in Tg-MI (Figure 7A). In addition, DNA ladder appeared faint in the noninfarcted LV from Tg-MI compared with that from WT-MI, suggesting the attenuation of apoptosis by *TFAM* overexpression (Figure 7B).

Discussion

The present study provides the first direct evidence that the overexpression of *TFAM* can prevent the decline in mtDNA as well as mitochondrial respiratory defects in post-MI hearts. TFAM significantly attenuated cardiac chamber dilatation and dysfunction as well as histopathological changes such as myocyte hypertrophy, interstitial fibrosis, and apoptosis. The apparent beneficial effects of *TFAM* overexpression were not due to its MI size–sparing effect, but they occurred secondary to more adaptive remodeling. All of these beneficial effects could contribute to the improved survival in Tg mice after MI.

Previous studies have suggested an intimate link between mtDNA damage, increased lipid peroxidation, and a decrease in mitochondrial electron transport complex enzyme activities.[4] A growing body of evidence suggests that mtDNA deficiencies and mitochondrial dysfunction play a major role in the development and progression of cardiac failure. A recent study from our laboratory demonstrated a decline in TFAM and mtDNA copy number in a murine heart failure model after MI.[9] These studies imply a relationship between TFAM, mtDNA copy

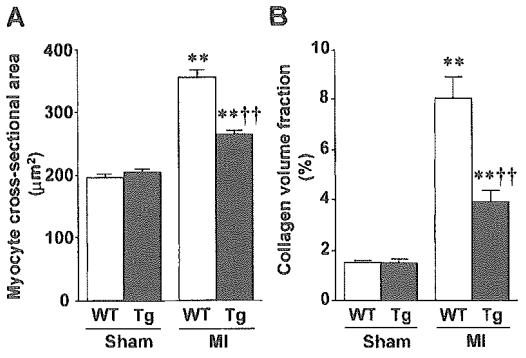

Figure 6. Summary data for histopathological analysis of LV tissue sections in 4 groups of animals (n=6 for each). Myocyte cross-sectional area (A) and collagen volume fraction (B) are shown. Values are mean±SEM. **$P<0.01$ for difference from WT-sham values; ††$P<0.01$ for difference from WT-MI values.

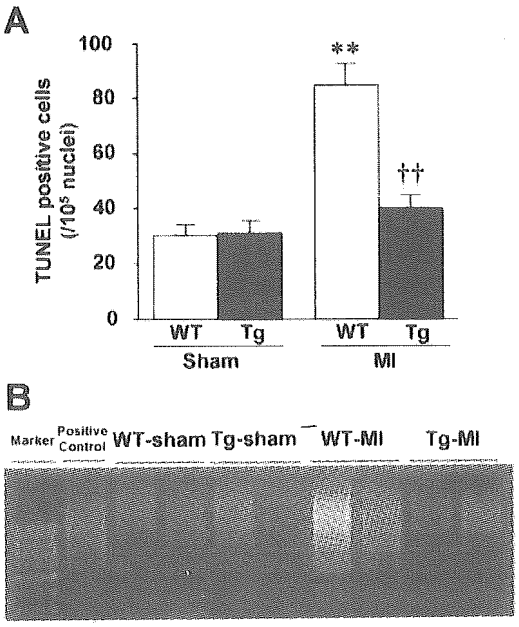

Figure 7. A, Number of TUNEL-positive myocytes in noninfarcted area of LV from 4 groups of animals (n=8 each). Values are mean±SEM. **$P<0.01$ for difference from WT-sham values. ††$P<0.01$ for difference from WT-MI values. B, DNA ladder indicative of apoptosis in genomic DNA from LV.

number, and mitochondrial function because the magnitude of the mtDNA defects is parallel to quantitative deficiencies in electron transport function. We thus proposed a direct relationship between TFAM content and electron transport chain activity during the post-MI remodeling process, ignoring the possibility of direct ischemic damage to the electron transport chain complexes. The downregulation of *TFAM* gene expression and a concurrent decrease in mitochondrial genes have been also shown in heart failure induced by aortic banding.[15] In addition, mtDNA depletion has been reported in mitochondrial myopathy and respiratory defects.[19–21] On the basis of these studies, mtDNA defects are considered to be involved not only in the pathogenesis of the diseases caused by inherited defects of mtDNA but also in those secondary to ischemia or mechanical overload.

TFAM not only regulates mtDNA transcription and replication[22] but also maintains mtDNA copy number. In fact, *Tfam* knockout mice, which had a 50% reduction in their transcript and protein levels, exerted a 34% reduction in the mtDNA copy number, 22% reduction in the mitochondrial transcript levels, and partial reduction in the cytochrome *c* oxidase levels in the heart.[11] Moreover, cardiac-specific disruption in the *Tfam* gene in mice exhibited dilated cardiomyopathy in association with a reduced amount of mtDNA and mitochondrial transcripts.[13] The transfection of antisense plasmids in culture, designed to reduce the expression of *TFAM*, effectively decreased the levels of mitochondrially encoded transcripts.[23] On the contrary, the forced overexpression of *TFAM* could produce the opposite effect.[24] Consistent with the present results (Figure 3A, 3B), a recent study by Ekstrand et al[25] demonstrated that the overexpression of human *TFAM* in the mouse increased mtDNA copy number. These lines of evidence imply the primary importance of TFAM as a regulatory mechanism of mtDNA copy number. TFAM has been shown to directly interact with mtDNA to form nucleoids.[26,27] Therefore, increased TFAM may increase the steady-state levels of mtDNA by directly binding and stabilizing mtDNA in Tg-sham mice. Our study also showed that overexpression of human *TFAM* did not increase the respiratory chain complex enzyme activities in Tg-sham mice (Figure 3C), suggesting that the regulation of mtDNA copy number is dissociated from that of electron transport function.[25] Furthermore, our proposed association between TFAM, mtDNA copy number, and electron transport chain activity may be weakened by our data that *TFAM* overexpression did not affect mtRNA levels (online-only Data Supplement I). There may be complex regulatory mechanisms responsible for the association of TFAM, mtDNA, and mitochondrial function, and further studies are clearly needed to solve this issue.

The results obtained from human *TFAM* Tg-sham mice differ from those from the inducible, cardiac-specific overexpression of peroxisome proliferator-activated receptor γ coactivator-1α (PGC-1α) transgene in adult mice, which leads to a modest increase in mitochondrial number and development of reversible cardiomyopathy.[28] PGC-1α is the transcriptional coactivator and acts upstream of TFAM and also has the capacity to increase mtDNA levels as well as mitochondrial mass in cultured cells and in Tg mice.[29,30] The reason for the discrepant results between PGC-1 and TFAM transgene overexpression remains unsolved in this study, which, however, may be related to the complex regulatory mechanisms of mitochondrial biogenesis and function by PGC-1 and its downstream factors, including nuclear respiratory factors 1 and 2 and TFAM.[31,32] This may also be due to the difference in the timing of transgene overexpression. Moreover, even though the present study demonstrated the beneficial effects of *TFAM* overexpression on post-MI LV remodeling, it could not determine whether it must occur before the ischemic insult or only during the post-MI phase.

The present study clearly demonstrated that *TFAM* overexpression could ameliorate the decline in mtDNA copy number and preserve it at a normal level in hearts from Tg-MI mice (Figure 3A). *TFAM* overexpression might increase the steady-state levels of mtDNA by directly stabilizing mtDNA. Consistent with alterations in mtDNA, the decrease in oxidative capacities seen in MI was also prevented (Figure 3B). Moreover, our studies establish an important role of TFAM in myocardial protection against remodeling and failure (Figures 4A and 5). The beneficial effects of *TFAM* overexpression shown in the present study were not due to its MI size–sparing effect because infarct size was comparable between WT-MI and Tg-MI mice (Figure 4B, 4C). Furthermore, its effects were not due to the effects on hemodynamics because blood pressure and heart rate were not altered (Table).

Several factors may be attributable to the protective effects conferred by TFAM against myocardial remodeling and failure. First, *TFAM* overexpression prevented the decrease in mtDNA copy number (Figure 3A) and mitochondrial electron transport function (Figure 3B), which may contribute to the decrease in myocardial oxidative stress. The decreased oxidative stress could contribute to the amelioration of cardiac hypertrophy, apoptosis, and interstitial fibrosis.[18] Second, *TFAM* overexpression may induce mitochondrial biogenesis, which, however, is thought to be unlikely because the number and size of the mitochondria assessed by electron microscopy were not altered in Tg-sham mice (online-only Data Supplement II). Importantly, the beneficial effects of *TFAM* overexpression on LV remodeling and failure occurred with the attenuation of increased mitochondrial number seen in MI. Furthermore, an increase in mitochondrial number itself did not necessarily exert beneficial effects in MI.

Several pathogenic mtDNA base substitution mutations, such as missense mutations and mtDNA rearrangement mutations (deletions and insertions), have been identified in patients with mitochondrial diseases.[4] An accumulation of the deleted forms of mtDNA in the myocardium frequently results in either cardiac hypertrophy, conduction block, or heart failure.[33] Furthermore, there is now a consensus view that mutations in mtDNA and abnormalities in mitochondrial function are associated with common forms of cardiac diseases, such as ischemic heart disease[34] and dilated cardiomyopathy.[35] In these conditions, however, the strict causal relationship between abnormalities in mtDNA and cardiac dysfunction has yet to be fully elucidated.

The present study supports our earlier conclusions that the deficiencies of mtDNA contribute to cardiac failure.[9] Furthermore, it confirms that the defects in TFAM are critically involved in mitochondrial dysfunction as well as maladaptive cardiac remodeling and failure. More importantly, the increased

TFAM expression could ameliorate the pathophysiological processes seen in heart failure. MtDNA decline and mitochondrial defects are now well recognized in a variety of diseases such as neurodegenerative diseases, diabetes mellitus, cancer, and even aging. Therefore, with further knowledge on the mechanisms of TFAM for maintenance of mtDNA copy number and mitochondrial function, it may eventually be possible to develop novel strategies for the treatment of such diseases based on the manipulation of TFAM.

Acknowledgments

This study was supported in part by grants from the Ministry of Education, Science, and Culture (Nos. 09670724, 12670676, 14370230). A part of this study was conducted in Kyushu University Station for Collaborative Research I and II.

References

1. Attardi G, Schatz G. Biogenesis of mitochondria. *Annu Rev Cell Biol.* 1988;4:289–333.
2. Shadel GS, Clayton DA. Mitochondrial DNA maintenance in vertebrates. *Annu Rev Biochem.* 1997;66:409–435.
3. Clayton DA. Replication and transcription of vertebrate mitochondrial DNA. *Annu Rev Cell Biol.* 1991;7:453–478.
4. Wallace DC. Mitochondrial diseases in man and mouse. *Science.* 1999; 283:1482–1488.
5. Kajander OA, Karhunen PJ, Jacobs HT. The relationship between somatic mtDNA rearrangements, human heart disease and aging. *Hum Mol Genet.* 2002;11:317–324.
6. Naya FJ, Black BL, Wu H, Bassel-Duby R, Richardson JA, Hill JA, Olson EN. Mitochondrial deficiency and cardiac sudden death in mice lacking the MEF2A transcription factor. *Nat Med.* 2002;8:1303–1309.
7. Lebrecht D, Setzer B, Ketelsen UP, Haberstroh J, Walker UA. Time-dependent and tissue-specific accumulation of mtDNA and respiratory chain defects in chronic doxorubicin cardiomyopathy. *Circulation.* 2003; 108:2423–2429.
8. Ide T, Tsutsui H, Kinugawa S, Utsumi H, Kang D, Hattori N, Uchida K, Arimura K, Egashira K, Takeshita A. Mitochondrial electron transport complex I is a potential source of oxygen free radicals in the failing myocardium. *Circ Res.* 1999;85:357–363.
9. Ide T, Tsutsui H, Hayashidani S, Kang D, Suematsu N, Nakamura K, Utsumi H, Hamasaki N, Takeshita A. Mitochondrial DNA damage and dysfunction associated with oxidative stress in failing hearts after myocardial infarction. *Circ Res.* 2001;88:529–535.
10. Parisi MA, Clayton DA. Similarity of human mitochondrial transcription factor 1 to high mobility group proteins. *Science.* 1991;252:965–969.
11. Larsson NG, Wang J, Wilhelmsson H, Oldfors A, Rustin P, Lewandoski M, Barsh GS, Clayton DA. Mitochondrial transcription factor A is necessary for mtDNA maintenance and embryogenesis in mice. *Nat Genet.* 1998;18:231–236.
12. Li H, Wang J, Wilhelmsson H, Hansson A, Thoren P, Duffy J, Rustin P, Larsson NG. Genetic modification of survival in tissue-specific knockout mice with mitochondrial cardiomyopathy. *Proc Natl Acad Sci U S A.* 2000;97:3467–3472.
13. Wang J, Wilhelmsson H, Graff C, Li H, Oldfors A, Rustin P, Bruning JC, Kahn CR, Clayton DA, Barsh GS, Thoren P, Larsson NG. Dilated cardiomyopathy and atrioventricular conduction blocks induced by heart-specific inactivation of mitochondrial DNA gene expression. *Nat Genet.* 1999;21:133–137.
14. Kanazawa A, Nishio Y, Kashiwagi A, Inagaki H, Kikkawa R, Horiike K. Reduced activity of mtTFA decreases the transcription in mitochondria isolated from diabetic rat heart. *Am J Physiol.* 2002;282:E778–E785.
15. Garnier A, Fortin D, Delomenie C, Momken I, Veksler V, Ventura-Clapier R. Depressed mitochondrial transcription factors and oxidative capacity in rat failing cardiac and skeletal muscles. *J Physiol.* 2003;551: 491–501.
16. Niwa H, Yamamura K, Miyazaki J. Efficient selection for high-expression transfectants with a novel eukaryotic vector. *Gene.* 1991;108: 193–199.
17. Shiomi T, Tsutsui H, Hayashidani S, Suematsu N, Ikeuchi M, Wen J, Ishibashi M, Kubota T, Egashira K, Takeshita A. Pioglitazone, a peroxisome proliferator–activated receptor-gamma agonist, attenuates left ventricular remodeling and failure after experimental myocardial infarction. *Circulation.* 2002;106:3126–3132.
18. Shiomi T, Tsutsui H, Matsusaka H, Murakami K, Hayashidani S, Ikeuchi M, Wen J, Kubota T, Utsumi H, Takeshita A. Overexpression of glutathione peroxidase prevents left ventricular remodeling and failure after myocardial infarction in mice. *Circulation.* 2004;109:544–549.
19. Moraes CT, Shanske S, Tritschler HJ, Aprille JR, Andreetta F, Bonilla E, Schon EA, DiMauro S. mtDNA depletion with variable tissue expression: a novel genetic abnormality in mitochondrial diseases. *Am J Hum Genet.* 1991;48:492–501.
20. Lewis W, Gonzalez B, Chomyn A, Papoian T. Zidovudine induces molecular, biochemical, and ultrastructural changes in rat skeletal muscle mitochondria. *J Clin Invest.* 1992;89:1354–1360.
21. Marin-Garcia J, Goldenthal MJ. Mitochondrial cardiomyopathy: molecular and biochemical analysis. *Pediatr Cardiol.* 1997;18:251–260.
22. Scarpulla RC. Nuclear activators and coactivators in mammalian mitochondrial biogenesis. *Biochim Biophys Acta.* 2002;1576:1–14.
23. Inagaki H, Kitano S, Lin KH, Maeda S, Saito T. Inhibition of mitochondrial gene expression by antisense RNA of mitochondrial transcription factor A (mtTFA). *Biochem Mol Biol Int.* 1998;45:567–573.
24. Montoya J, Perez-Martos A, Garstka HL, Wiesner RJ. Regulation of mitochondrial transcription by mitochondrial transcription factor A. *Mol Cell Biochem.* 1997;174:227–230.
25. Ekstrand MI, Falkenberg M, Rantanen A, Park CB, Gaspari M, Hultenby K, Rustin P, Gustafsson CM, Larsson NG. Mitochondrial transcription factor A regulates mtDNA copy number in mammals. *Hum Mol Genet.* 2004;13:935–944.
26. Alam TI, Kanki T, Muta T, Ukaji K, Abe Y, Nakayama H, Takio K, Hamasaki N, Kang D. Human mitochondrial DNA is packaged with TFAM. *Nucleic Acids Res.* 2003;31:1640–1645.
27. Takamatsu C, Umeda S, Ohsato T, Ohno T, Abe Y, Fukuoh A, Shinagawa H, Hamasaki N, Kang D. Regulation of mitochondrial D-loops by transcription factor A and single-stranded DNA-binding protein. *EMBO Rep.* 2002;3:451–456.
28. Russell LK, Mansfield CM, Lehman JJ, Kovacs A, Courtois M, Saffitz JE, Medeiros DM, Valencik ML, McDonald JA, Kelly DP. Cardiac-specific induction of the transcriptional coactivator peroxisome proliferator-activated receptor gamma coactivator-1alpha promotes mitochondrial biogenesis and reversible cardiomyopathy in a developmental stage-dependent manner. *Circ Res.* 2004;94:525–533.
29. Lin J, Wu H, Tarr PT, Zhang CY, Wu Z, Boss O, Michael LF, Puigserver P, Isotani E, Olson EN, Lowell BB, Bassel-Duby R, Spiegelman BM. Transcriptional co-activator PGC-1 alpha drives the formation of slow-twitch muscle fibres. *Nature.* 2002;418:797–801.
30. Wu Z, Puigserver P, Andersson U, Zhang C, Adelmant G, Mootha V, Troy A, Cinti S, Lowell B, Scarpulla RC, Spiegelman BM. Mechanisms controlling mitochondrial biogenesis and respiration through the thermogenic coactivator PGC-1. *Cell.* 1999;98:115–124.
31. Huss JM, Kelly DP. Nuclear receptor signaling and cardiac energetics. *Circ Res.* 2004;95:568–578.
32. Ventura-Clapier R, Garnier A, Veksler V. Energy metabolism in heart failure. *J Physiol.* 2004;555:1–13.
33. Anan R, Nakagawa M, Miyata M, Higuchi I, Nakao S, Suehara M, Osame M, Tanaka H. Cardiac involvement in mitochondrial diseases: a study on 17 patients with documented mitochondrial DNA defects. *Circulation.* 1995;91:955–961.
34. Corral-Debrinski M, Shoffner JM, Lott MT, Wallace DC. Association of mitochondrial DNA damage with aging and coronary atherosclerotic heart disease. *Mutat Res.* 1992;275:169–180.
35. Arbustini E, Diegoli M, Fasani R, Grasso M, Morbini P, Banchieri N, Bellini O, Dal Bello B, Pilotto A, Magrini G, Campana C, Fortina P, Gavazzi A, Narula J, Vigano M. Mitochondrial DNA mutations and mitochondrial abnormalities in dilated cardiomyopathy. *Am J Pathol.* 1998;153:1501–1510.

Adenovirus-Mediated Overexpression of Diacylglycerol Kinase-ζ Inhibits Endothelin-1–Induced Cardiomyocyte Hypertrophy

Hiroki Takahashi, MD; Yasuchika Takeishi, MD; Tim Seidler, MD; Takanori Arimoto, MD; Hideyuki Akiyama, MD; Yasukazu Hozumi, MD; Yo Koyama, MD; Tetsuro Shishido, MD; Yuichi Tsunoda, MD; Takeshi Niizeki, MD; Naoki Nozaki, MD; Jun-ichi Abe, MD; Gerd Hasenfuss, MD; Kaoru Goto, MD; Isao Kubota, MD

Background—Diacylglycerol (DAG) is a lipid second messenger that transiently accumulates in cells stimulated by endothelin-1 (ET-1) and other Gαq protein-coupled receptor agonists. Diacylglycerol kinase (DGK) is thought to be an enzyme that controls the cellular levels of DAG by converting it to phosphatidic acid; however, the functional role of DGK has not been examined in cardiomyocytes. Because DGK inactivates DAG, a strong activator of protein kinase C (PKC), we hypothesized that DGK inhibited ET-1–induced activation of a DAG-PKC signaling cascade and subsequent cardiomyocyte hypertrophy.

Methods and Results—Real-time reverse transcription–polymerase chain reaction demonstrated a significant increase of DGK-ζ mRNA by ET-1 in cardiomyocytes. To determine the functional role of DGK-ζ, we overexpressed DGK-ζ in cardiomyocytes using a recombinant adenovirus encoding rat DGK-ζ (Ad-DGKζ). ET-1–induced translocation of PKC-ε was blocked by Ad-DGKζ ($P<0.01$). Ad-DGKζ also inhibited ET-1–induced activation of extracellular signal–regulated kinase ($P<0.01$). Luciferase reporter assay revealed that ET-1–mediated increase of activator protein-1 (AP1) DNA-binding activity was significantly inhibited by DGK-ζ ($P<0.01$). In cardiomyocytes transfected with DGK-ζ, ET-1 failed to cause gene induction of atrial natriuretic factor, increases in [^{3}H]-leucine uptake, and increases in cardiomyocyte surface area.

Conclusions—We demonstrated for the first time that DGK-ζ blocked ET-1–induced activation of the PKC-ε–ERK-AP1 signaling pathway, atrial natriuretic factor gene induction, and resultant cardiomyocyte hypertrophy. DGK-ζ might act as a negative regulator of hypertrophic program in response to ET-1, possibly by controlling cellular DAG levels. **(*Circulation*. 2005;111:1510-1516.)**

Key Words: signal transduction ■ hypertrophy ■ enzymes ■ proteins ■ endothelin

Cardiac hypertrophy is a major risk factor for the development of heart failure and death.[1] Identification of the signaling molecules involved in the progression of cardiac hypertrophy may lead to the development of therapeutic strategies to prevent heart failure. It has been widely recognized that heterotrimeric $G_{\alpha q}$ protein–coupled receptor agonists such as endothelin-1 (ET-1), angiotensin II, phenylephrine, and others play an important role in the development of cardiac hypertrophy and progression of heart failure.[2] In addition, there is substantial evidence to indicate a critical role of overactivity of the $G_{\alpha q}$ protein–coupled receptor signaling pathway.[3] Ligand binding to its cognate 7 transmembrane-spanning receptor activates phospholipase C-β1 and causes cleavage of membrane-bound phosphatidylinositol biphosphate into diacylglycerol (DAG) and inositol 1,4,5-triphosphate.[4] DAG is a lipid second messenger and functions as a strong activator of protein kinase C (PKC).[5] PKC is a serine-threonine kinase and modulates a variety of cellular functions, including gene transcription, voltage-dependent Ca^{2+} channel, Na^+/H^+ exchanger, sarcoplasmic reticular proteins, and myofilament proteins.[6] Previous studies in human heart failure and animal models of heart failure that included genetically engineered mice clearly demonstrated that activation of PKC plays a pivotal role in the development of cardiac hypertrophy and heart failure.[7–11]

DAG kinase (DGK) is an enzyme that is responsible for controlling the cellular levels of DAG by converting it to phosphatidic acid[12] and thus is thought to act as an endoge-

Received July 19, 2004; revision received November 15, 2004; accepted November 29, 2004.

From First Department of Internal Medicine (H.T., Y. Takeishi, T.A., H.A., Y.K., T. Shishido, Y. Tsunoda, T.N., N.N., I.K.) and Department of Anatomy and Cell Biology (H.A., Y.H., K.G.), Yamagata University School of Medicine, Yamagata, Japan; Department of Cardiology and Pneumology (T. Seidler, G.H.), Georg-August-University Goettingen, Goettingen, Germany; and Center for Cardiovascular Research (J.A.), University of Rochester, Rochester, NY.

Correspondence to Yasuchika Takeishi, MD, First Department of Internal Medicine, Yamagata University School of Medicine, 2-2-2 Iida-Nishi, Yamagata, Japan 990-9585. E-mail takeishi@med.id.yamagata-u.ac.jp

Circulation is available at http://www.circulationaha.org

DOI: 10.1161/01.CIR.0000159339.00703.22

nous regulator of PKC activity. To date, 9 mammalian DGK isoforms, which differ in tissue expression and structural domains, have been identified.[13,14] A previous study has indicated that 3 DGK isoforms (DGK-α, DGK-ε, and DGK-ζ) are expressed in adult rat myocardium,[15] and the DGK-ζ isoform is predominant; however, the functional role of DGK isoforms in cardiomyocytes remains unclear.

Therefore, in the present study, to clarify the potential roles of DGK-ζ in the cardiomyocyte, DGK-ζ was transiently overexpressed into cultured rat neonatal cardiomyocytes with a recombinant adenovirus that encodes rat DGK-ζ. We studied the effects of DGK-ζ on ET-1–induced activation of DAG-PKC signaling and resultant cardiomyocyte hypertrophy.

Methods

Materials and Reagents

ET-1, BQ-123, and BQ-788 were purchased from Sigma-Aldrich Japan. [^{3}H]-leucine was purchased from Amersham Biosciences Corp. Collagenase A, Fugene 6, and LightCycler DNA Master SYBR Green I were obtained from Roche Diagnostics Japan. The Dual-Luciferase Reporter Assay System and *phRL-TK* were purchased from Promega Corporation. *pAP1-Luc* plasmid was obtained from Stratagene. Antibodies for extracellular signal–regulated kinase (ERK) and PKC isoforms were obtained from Cell Signaling Technology, Inc, and BD Transduction Laboratories, respectively. All other chemicals were purchased from Invitrogen Corp.

Cardiomyocyte Isolation and Culture

The animals were handled according to the animal welfare regulations of Yamagata University, and the study protocol was approved by the Animal Subjects Committee of Yamagata University. The investigation conformed with the *Guide for the Care and Use of Laboratory Animals* published by the US National Institutes of Health.

Cultured rat neonatal cardiomyocytes were prepared as described previously.[16] Briefly, ventricles were obtained from 1- or 2-day-old Sprague-Dawley rats, and cardiomyocytes were isolated by digestion with collagenase. Cardiomyocytes were kept in serum-free medium (control medium) supplemented with transferrin (5 mg/mL) and insulin (1 mg/mL) for 24 hours before adenoviral infection. In this study, to induce cardiomyocyte hypertrophy, ET-1 (100 nmol/L) was added in the control medium, and cells were incubated for 48 hours.[17] In some experiments, selective ET_A receptor antagonist BQ-123 (10 μmol/L) or selective ET_B receptor antagonist BQ-788 (10 μmol/L) was added to the medium 1 hour before the addition of ET-1.[18]

Adenoviral Overexpression of DGK-ζ in Isolated Rat Neonatal Cardiomyocytes

The rat DGK-ζ gene[19,20] in vector pcDNA3.1 was cloned and ligated downstream from an immediate-early cytomegalovirus promoter into vector pACCMV.pLpA with primers to create *Kpn*I and *Hind*III sites (Ad-DGKζ). Recombination with pJM17 plasmid and production of replication-deficient adenovirus were performed according to standard procedures as reported previously.[21] Gene transfer with adenovirus encoding β-galactosidase (Ad-LacZ) was used as an internal control.

Luciferase Assays

The plasmid *pAP1-Luc* that contained the firefly luciferase reporter gene driven by a basic promoter element (TATA box) joined to tandem repeats of activator protein-1 (AP1) binding element was obtained from Stratagene. As an internal control, *phRL-TK* that contained the renilla luciferase reporter gene driven by the herpes simplex virus–thymidine kinase promoter was used. At 24 hours after DGK transfection, cardiomyocytes were cotransfected with *pAP1-Luc* and *phRL-TK* using Fugene 6 as reported previously.[22] After the preconditioning period of 24 hours, ET-1 or vehicle was added to the culture medium for 12 hours. Both firefly and renilla luciferase activities were determined in the same cell lysates with the Dual-Luciferase Reporter Assay System and MiniLumat LB9506 (Perkin-Elmer Japan Co, Ltd). Each firefly luciferase activity as AP1 transcriptional activity was corrected for differences in transfection efficiency by division with the renilla luciferase luminometric signal from the same well.[22]

Western Blotting for ERK Phosphorylation Activity

Cardiomyocytes were lysed in ice-cold lysis buffer, and the protein was extracted as reported previously.[23,24] To examine phosphorylation activity of ERK, Western blotting was performed with an anti-phosphospecific ERK1/2 antibody as reported previously.[23,24] To quantify the protein levels, the same membranes were reprobed with nonspecific anti-ERK1/2 antibody. The relative amount of phosphorylated proteins versus total proteins was used for phosphorylation kinase activity.

Protein Extraction and Separation of Membranous and Cytosolic Fractions for PKC Localization

Protein samples were extracted from the cardiomyocyte, and membranous and cytosolic fractions of detergent-extracted PKC were prepared as described previously.[9,10,24] Equal amounts of membranous and cytosolic protein were subjected to electrophoresis, and the subcellular localization of PKC isoforms was examined by quantitative immunoblotting with isoform-specific antibodies as reported previously.[9,10,24] Membrane/cytosol ratios of immunoreactivity were used as indices for the extent of translocation of PKC isoforms.[9,10,24]

Assessment of Cardiomyocyte Hypertrophy

After 48 hours' incubation with ET-1, we measured cell surface areas using the Scion Image (Scion Corporation) as reported previously.[25] At least 100 cardiomyocytes in 20 to 25 fields were examined in each experiment, and the data were averaged.

The rate of protein synthesis was determined by incorporation of [^{3}H]-leucine as described previously.[26] Briefly, cardiomyocytes (1.0×10^5 cells/cm^2) were stimulated with ET-1 in medium supplemented with [^{3}H]-leucine (1.0 μCi/mL). Thereafter, the cells were rinsed 3 times with ice-cold PBS and treated with 5% trichloroacetic acid (TCA) on ice for 20 minutes. After they were washed twice with ice-cold 5% TCA, cells were lysed in 0.5 N NaOH. The lysate was neutralized by 0.5 N HCl, and OPTI-FLOUR (Perkin-Elmer Japan Co, Ltd) was applied. The incorporation of [^{3}H]-leucine was measured by a Tri-Carb Liquid Scintillation Analyzer (Perkin-Elmer Japan).

Extraction of Total RNA and Real-Time Reverse Transcription-Polymerase Chain Reaction

Total RNA was extracted from cardiomyocytes with TRIzol as described previously.[27] First-strand cDNA was synthesized from 1 μg of RNA sample with oligo (dT) primers and superscript II reverse transcriptase. Real-time polymerase chain reaction (PCR) was performed with LightCycler DNA Master SYBR Green I in a 20-μL volume reaction with a light cycler (Roche Diagnostics Japan). Standard curves of DGK-ζ and atrial natriuretic factor (ANF) amplification were generated by full-sequence plasmids of known concentrations, respectively. Variability in the initial quantities of cDNA was normalized to GAPDH. The primers used for amplification were 5′-GAAGTTCAACAGCCGCTTTC-3′ (forward) and 5′-AGAGCCTCGTAGTCGTGCAT-3′ (reverse) for DGK-ζ, and 5′-GATGGATTTCAAGAACCTGC-3′ (forward) and 5′-TTCAAGAGGGCAGATCTATC-3′ (reverse) for ANF.[15,25]

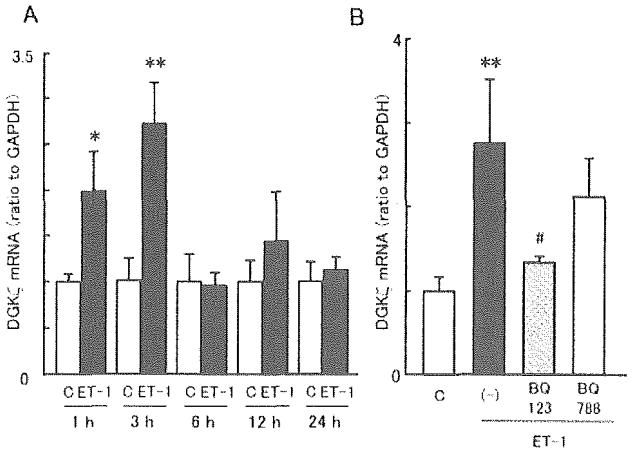

Figure 1. A, Quantitative analysis of DGK-ζ mRNA expression after ET-1 stimulation in rat neonatal cardiomyocytes. mRNA levels for DGK-ζ were examined by real-time RT-PCR and normalized to GAPDH. Open bars indicate control (C), and solid bars indicate ET-1 data. B, Effects of selective ET-1 receptor antagonists on DGK-ζ mRNA expression. Selective ET_A receptor antagonist BQ-123 or selective ET_B receptor antagonist BQ-788 was added to medium 1 hour before addition of ET-1. Values are mean±SEM (n=10). *$P<0.05$ and **$P<0.01$ vs control; #$P<0.05$ vs ET-1.

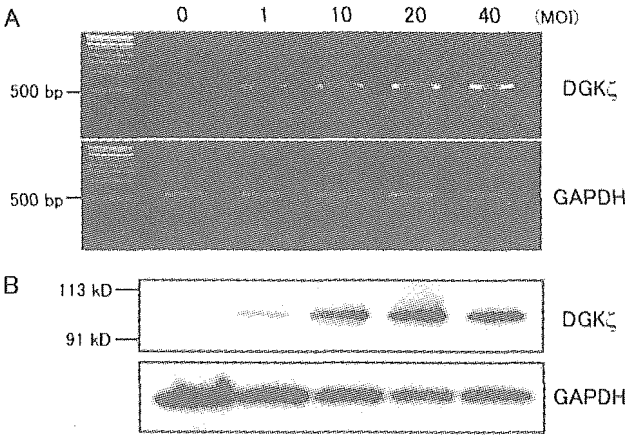

Figure 2. Verification of transgene expression in isolated rat neonatal cardiomyocytes. Forty-eight hours after transfection with indicated multiplicity of infection (MOI), RT-PCR (A) and immunoblots (B) indicate successful overexpression of DGK-ζ mRNA and protein, respectively. Detection of GAPDH served to demonstrate equal sample loading.

Statistical Analysis

Data are expressed as mean±SEM. Comparisons among groups were performed by 1-way ANOVA followed by Fisher's protected least significant difference test. Values with $P<0.05$ were considered statistically significant.

Results

Quantitative Analysis of DGK-ζ mRNA Expression After ET-1 Stimulation

Whether DGK-ζ mRNA expression is changed after stimulation with hypertrophic agonists in cardiomyocytes has not been examined previously. To quantitatively determine changes in mRNA levels of DGK-ζ after ET-1 stimulation, we performed real-time reverse transcription (RT)-PCR analysis. As shown in Figure 1A, DGK-ζ mRNA levels increased significantly at 1 hour (1.98±0.43-fold, $P<0.05$) and 3 hours (2.93±0.45-fold, $P<0.01$) after ET-1 stimulation and returned to basal levels after 6 hours. These results suggest that ET-1 upregulated DGK-ζ mRNA expression in rat neonatal cardiomyocytes.

To identify which ET receptor subtype was responsible for the induction of DGK-ζ mRNA, we examined the effects of selective antagonists for ET_A (BQ123) and ET_B (BQ788) on ET-1–induced DGK-ζ mRNA expression. ET-1–induced increases in DGK-ζ mRNA expression were significantly inhibited by treatment with BQ123 but not by BQ788 (Figure 1B). These observations suggested that ET-1 increased DGK-ζ mRNA expression via the ET_A receptor in cardiomyocytes.

Adenovirus-Mediated Expression of DGK-ζ in Rat Neonatal Cardiomyocytes

To examine the effect of DGK-ζ on subcellular signaling and cardiomyocyte hypertrophy, rat neonatal cardiomyocytes were transfected with a recombinant adenovirus encoding for rat DGK-ζ (Ad-DGKζ). After incubation of cardiomyocytes with Ad-DGKζ for 48 hours, RT-PCR and immunoblots were performed to confirm the adenovirus-mediated expression of DGK-ζ. As shown in Figures 2A and 2B, mRNA and protein levels of DGK-ζ rose in a dose-dependent manner. On the basis of these results, cardiomyocytes 48 hours after transfection with 20 multiplicity of infection (MOI) Ad-DGKζ were used for the following experiments.

Inhibition of ET-1–Induced PKC-ε Translocation in Cardiomyocytes by DGK-ζ

It has been reported that ET-1, a potent hypertrophic agonist, causes the translocation of PKC-ε to the membrane fraction in rat neonatal cardiomyocytes.[28] Therefore, we examined the effects of Ad-DGKζ or Ad-LacZ on ET-1–induced translocation of PKC isoforms in cardiomyocytes using isoform-specific antibodies. As shown in Figure 3, the membrane-associated immunoreactivity of the PKC-ε isoform was significantly increased in ET-1–stimulated cardiomyocytes after Ad-LacZ transfection. However, translocation of PKC-α and PKC-δ by ET-1 was not observed in our cardiomyocyte preparations (Figures 3A and 3B). ET-1–induced translocation of PKC-ε was blocked after Ad-DGKζ transfection (membrane/cytosol ratio 4.93±0.35 versus 1.31±0.14, $P<0.01$), as shown in Figure 3C. These data suggest that DGK-ζ had an inhibitory effect on ET-1–induced PKC-ε translocation in cardiomyocytes.

Inhibition of ET-1–Induced ERK Activation by DGK-ζ

We next investigated effects of Ad-DGKζ on ET-1–induced ERK activation. As shown in Figure 4, we observed significant ERK activation in ET-1–stimulated cardiomyocytes after Ad-LacZ transfection (3.39±1.05-fold over control, $P<0.01$); however, after Ad-DGKζ transfection, ET-1–induced ERK activation was completely abolished (0.78±0.20-fold, $P<0.01$). Equal protein levels of ERK were demonstrated among cardiomyocytes infected with Ad-DGKζ or Ad-LacZ, as shown in Figure 4. These results suggest the

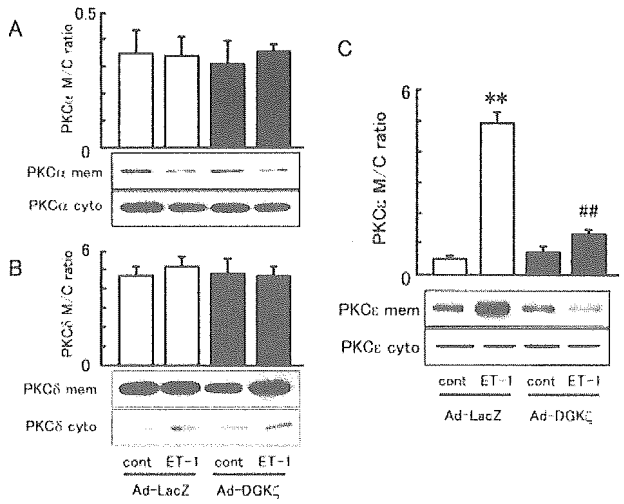

Figure 3. Changes in subcellular localization of PKC isoforms were examined by quantitative immunoblotting with isoform-specific antibody. Membrane/cytosol ratio (M/C ratio) of immunoreactivity was used as index of PKC translocation. Representative immunoblots and group data for M/C ratio of PKC-α (A) and PKC-δ (B) in response to ET-1. Translocation of PKC-α and PKC-δ was not observed after ET-1 in this cardiomyocyte preparation. C, Representative immunoblots and M/C ratio for translocation of PKC-ε. ET-1 translocated PKC-ε to membranous fraction, and this translocation was blocked by Ad-DGKζ. Data are mean±SEM and were obtained from 6 separate experiments for each group. **$P<0.01$ vs control Ad-LacZ; ##$P<0.01$ vs ET-1 Ad-LacZ. cont indicates control; mem, membrane; and cytosol.

inhibitory effect of DGK-ζ on ET-1–induced ERK activation in cardiomyocytes.

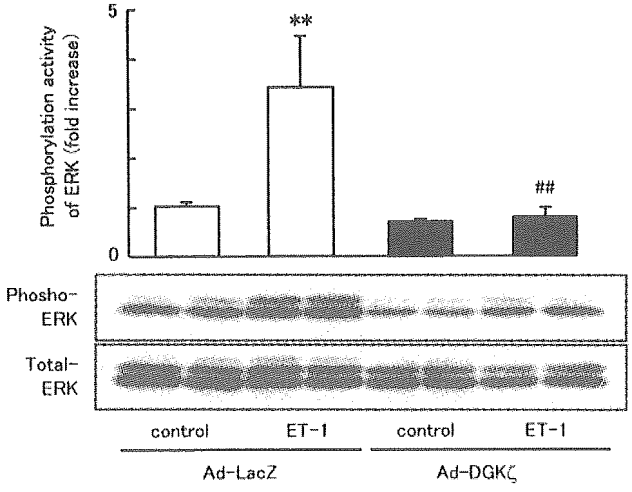

Figure 4. Inhibition of ET-1–induced ERK activation by Ad-DGKζ. Changes in phosphorylation activity of ERK were measured by Western blotting with phosphospecific ERK antibody (upper blots). No difference in amount of total ERK protein was observed in lysates from any samples by Western blot analysis with anti-ERK antibody (lower blots). Results were normalized for all experiments by arbitrarily setting densitometry of control Ad-LacZ samples to 1.0 (n=8). **$P<0.01$ vs control Ad-LacZ; ##$P<0.01$ vs ET-1 Ad-LacZ.

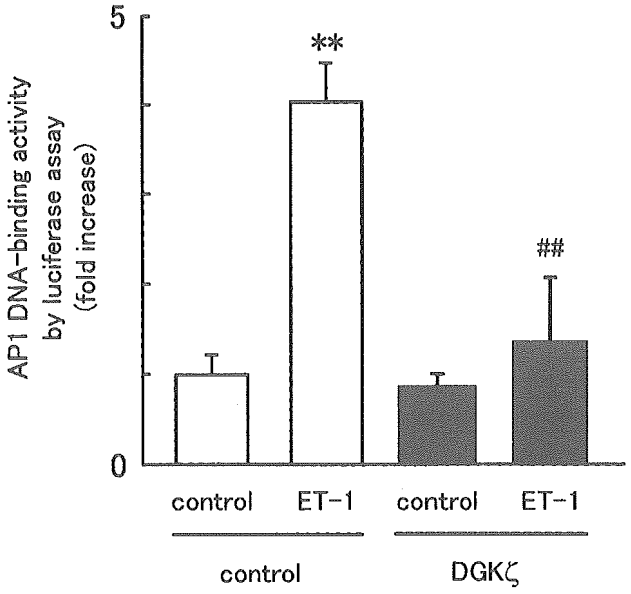

Figure 5. Inhibition of ET-1–induced AP1 DNA-binding activity by DGK-ζ. Cardiomyocytes were transfected with *pAP1-Luc* and *phRL-TK*. Each AP1 luciferase luminometric value was corrected for process differences by division with *phRL-TK* luciferase luminometric signal from same well. Bar graph with error bars represents mean±SEM (n=12). **$P<0.01$ vs control; ##$P<0.01$ vs ET-1.

Inhibition of ET-1–Induced AP1 DNA-Binding Activity

ET-1–induced activation of the PKC-ε–ERK pathway leads to activation of the AP1 transcription factor, thereby promoting the transcription of immediate-early genes such as c-fos and c-jun.[24] Therefore, we investigated whether DGK-ζ inhibited ET-1–induced activation of AP1 DNA-binding activity by luciferase assay. As shown in Figure 5, AP1 DNA-binding activity was significantly increased in ET-1–stimulated cardiomyocytes (4.14±0.22-fold, $P<0.01$). After transfection of DGK-ζ, ET-1 did not increase AP1 DNA-binding activity, as shown in Figure 5 (1.36±0.72-fold, $P<0.01$). These results suggest the inhibitory effect of DGK-ζ on ET-1–induced AP1 DNA-binding activity.

Effects of DGK-ζ on Hypertrophic Responses to ET-1

We then examined the effects of Ad-DGKζ or Ad-LacZ on hypertrophic responses to ET-1 determined by the induction of hypertrophic gene ANF, protein synthesis, and increases in cardiomyocyte surface area. Real-time RT-PCR revealed that ET-1 induced ANF gene expression after Ad-LacZ transfection (2.67±0.82-fold, $P<0.01$); however, Ad-DGKζ inhibited ET-1–induced increases in ANF gene expression levels, as shown in Figure 6A (1.13±0.20-fold, $P<0.01$).

Figure 6B shows the protein synthesis evaluated by the incorporation of [^{3}H]-leucine into cultured cardiomyocytes. Although ET-1 augmented [^{3}H]-leucine uptake (1.33±0.06-fold, $P<0.01$) in control cardiomyocytes, ET-1 did not increase [^{3}H]-leucine uptake (1.11±0.07-fold, $P<0.01$) in cardiomyocytes infected with Ad-DGKz.

Furthermore, we measured cardiomyocyte areas after Ad-DGKζ or Ad-LacZ transfection. As shown in Figure 7, ET-1

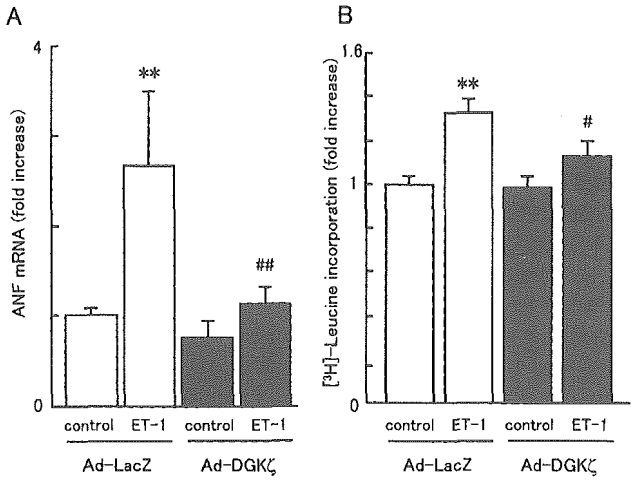

Figure 6. A, Effects of Ad-DGKζ on ANF gene induction by ET-1. B, Effects of Ad-DGKζ on ET-1–induced increases in incorporation of [^{3}H]-leucine. Data reported are mean±SEM from 3 independent experiments. Ad-DGKζ blocked ET-1–induced ANF gene induction and increases in [^{3}H]-leucine uptake. $^{**}P<0.01$ vs control Ad-LacZ; $\#P<0.05$ and $\#\#P<0.01$ vs ET-1 Ad-LacZ.

stimulation for 48 hours caused enlargement of cardiomyocyte surface area infected with Ad-LacZ (2486±57 versus 3113±64 μm^2, $P<0.01$); however, after transfection of Ad-DGKζ, ET-1 did not cause increases in cardiomyocyte surface area (2653±59 μm^2, $P<0.01$). These results suggest that DGK-ζ blocked hypertrophic responses by ET-1.

Discussion

We demonstrated that adenovirus-mediated overexpression of DGK-ζ inhibited the ability of ET-1 to induce the cardiomyocyte hypertrophic growth program. In cardiomyocytes transfected with Ad-DGKζ, ET-1 failed to induce translocation of PKC-ε, ERK activation, AP1 DNA-binding activation, ANF gene induction, and subsequent increases in [^{3}H]-leucine uptake and cardiomyocyte surface area.

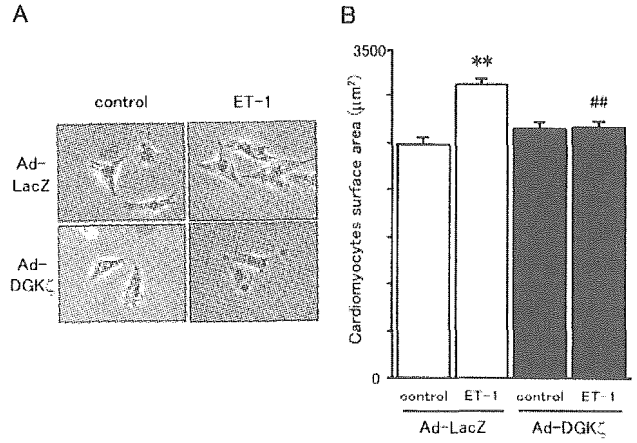

Figure 7. A, Light microscopic observations. Cardiomyocytes were infected with Ad-DGKζ or Ad-LacZ and then treated with ET-1. Representative cardiomyocytes are demonstrated. B, Effects of Ad-DGKζ on ET-1–induced increases in cardiomyocyte surface area. At least 100 cardiomyocytes in 20 to 25 fields were examined in each experiment, and values were averaged. Data reported are mean±SEM from 6 independent experiments. $^{**}P<0.01$ vs control Ad-LacZ; $\#\#P<0.01$ vs ET-1 Ad-LacZ.

Increases of DGK-ζ mRNA by ET-1 in Rat Neonatal Cardiomyocytes

DGK is a well-conserved lipid kinase that phosphorylates DAG to yield phosphatidic acid and is therefore thought to be an endogenous regulator of DAG-PKC signaling.[13] To date, 9 mammalian DGK isoforms have been cloned and divided into 5 classes based on common structural motifs.[14] DGK-ζ has been isolated from cDNA libraries of rat retina and brain.[19] In adult rat myocardium, it has been reported that DGK-ζ mRNA level is increased in the area of experimental myocardial infarction in the acute phase[15]; that study concluded that this increase of DGK-ζ mRNA in the infarct area might be ascribed to infiltrated macrophages and granulocytes. In the present study, we demonstrated that ET-1 increased mRNA levels of DGK-ζ in isolated rat neonatal cardiomyocytes. To the best of our knowledge, this is the first report showing that DGK-ζ mRNA expression is upregulated by a hypertrophic agonist in cardiomyocytes.

We also demonstrated that ET-1 increased mRNA levels of DGK-ζ via the ET_A receptor but not the ET_B receptor in cardiomyocytes (Figure 1). It has been reported that cardiomyocytes predominantly express the ET_A receptor.[29] Consistent with expression levels in cardiomyocytes, the ET_A receptor acts as a major pathway for several effects of ET-1, including myocardial contraction and hypertrophy.[30] Similarly, ET-1–induced DGK-ζ mRNA expression in cardiomyocytes was mediated via the ET_A receptor in the present study. These data support the notion that DGK may play a role in regulating hypertrophic growth in response to $G_{\alpha q}$ protein–coupled receptor agonists or other mechanical stimuli.

Critical Role of the DAG-PKC Signaling Pathway

It has been reported that ET-1 causes membrane translocation of PKC-ε, and to a lesser extent PKC-δ, in cultured rat neonatal cardiomyocytes.[28] ET-1–induced PKC-ε translocation is accompanied by subsequent activation of ERK.[4] In animal models of cardiac hypertrophy and heart failure by pressure overload, translocation and activation of PKC-α and PKC-ε isoforms are observed.[9,24] We have demonstrated that transgenic overexpression of a constitutively active mutant of the PKC-ε isoform in the mouse heart results in concentric cardiac hypertrophy.[11] Conversely, overexpression of PKC-β2 in transgenic mouse heart causes a dilated cardiomyopathy phenotype.[7] Furthermore, activation of the Ca^{2+}-sensitive PKC-α, -β1, and -β2 isoforms is demonstrated in human end-stage heart failure.[8] Therefore, it is important to regulate PKC activity and its downstream signaling pathway in the development of cardiac hypertrophy and heart failure.

Effects of Phosphatidic Acid on Cardiomyocyte Hypertrophy

Phosphatidic acid is yielded not only by DGK but also by the action of phospholipase D. Phospholipase D hydrolyzes phosphatidylcholine to form phosphatidic acid, and phosphatidic acid itself also has a signaling function. It has been reported that phosphatidic acid stimulates DNA synthesis and

modulates the activity of several enzymes, including phosphatidylinositol-4-phosphate 5-kinases, ERK, and others.[13,31] However, because the bulk of the signaling pool of phosphatidic acid is derived from the action of phospholipase D,[32] overexpression of DGK-ζ may not affect the phosphatidic acid pool and its signaling function. Activation of downstream ERK and protein synthesis by ET-1 were abolished by Ad-DGKζ in the present study (Figures 4 and 6B). These results suggest the importance of inhibiting the DAG-PKC signaling pathway by DGK-ζ to prevent cardiomyocyte hypertrophy.

DGK as a Regulator of the DAG-PKC Signaling Pathway

DAG is a potent activator of conventional and novel PKC subfamilies.[4] As indicated in Figure 3, the PKC-ε isoform was translocated from a cytosolic to a membranous fraction by ET-1. The PKC-ε isoform belongs to the novel PKC subfamily, which is activated by DAG but not Ca^{2+}.[33] Previous studies have demonstrated the interconnectivity between PKC-ε and ERK signaling in cardiomyocytes.[17] The AP1 is a sequence-specific transcriptional activator composed of the Jun and Fos families. Recent studies have demonstrated that myocardial AP1 DNA-binding activities are involved in experimental cardiac hypertrophy.[34] ERK activation results in increased synthesis of c-Fos, which translocates to the nucleus and combines with preexisting c-Jun proteins to form AP1 dimers.[35]

Recently, it has been reported that PKC-α inhibits DGK-ζ in HEK293 cells.[36] Activated PKC-α phosphorylates DGK-ζ, and this phosphorylation inhibits DGK activity to remove cellular DAG. In the present study with rat neonatal cardiomyocytes, PKC-α was not activated by ET-1 (Figure 3A), and these results were concordant with previous reports.[28] Adenovirus-mediated overexpression of DGK-ζ also did not affect PKC-α translocation (Figure 3A).

In Jurkat T cells, Zhong et al[37] recently reported that overexpression of DGK-ζ interferes with T-cell antigen receptor-induced ERK activation and AP1 induction. Luo et al[38] have demonstrated spatial association of DGK-ζ with PKC-α in HEK293 cells. Recently, Verrier et al[39] demonstrated that peroxisome proliferator–activated receptor-γ agonists activate DGK-α mRNA expression and ameliorate endothelial cell activation via the inhibition of a DAG-PKC signaling pathway. However, the functional role of any DGK isoforms in the regulation of DAG-PKC signaling has not been investigated in cardiomyocytes. In the present study, we demonstrated for the first time that DGK-ζ inhibited the ET-1–induced hypertrophic growth program characterized by activation of the PKC-ERK-AP1 signaling pathway with resultant induction of ANF gene expression. Furthermore, DGK-ζ abolished increases in protein synthesis and cardiomyocyte surface area by ET-1. Thus, DGK-ζ may act as an inhibitor of a DAG-PKC signaling cascade in cardiomyocytes by controlling cellular DAG levels.

ET-1 is only one of the neurohumoral factors that mediate $G_{\alpha q}$ stimulation with resultant increases in cellular DAG levels.[3] Other $G_{\alpha q}$ protein–coupled receptor agonists, such as angiotensin II, phenylephrine, and prostaglandin $F_{2\alpha}$, also activate this cell signaling pathway by binding to their respective cognate 7 transmembrane spanning receptors.[4] Therefore, the control of cellular DAG levels by DGK-ζ might inhibit this signaling cascade more effectively than does the pharmacological blockade of each receptor.

Conclusions

The present data showed that DGK-ζ might act as a negative regulator of hypertrophic response via inhibition of the PKC-ε–ERK-AP1 pathway. Because $G_{\alpha q}$ protein–coupled receptor signaling plays an important role in the development of cardiac hypertrophy and the progression of heart failure, DGK-ζ might represent a new target for the prevention and treatment of this pathological process. Future experiments generating genetically manipulated mice will further elucidate the present results obtained from cultured cardiomyocytes.

Acknowledgments

This study was supported in part by grants-in-aid for scientific research (Nos. 14570635 and 16590657) from the Ministry of Education, Science, Sports and Culture, Japan, and grants from the Japan Foundation of Cardiovascular Research, The Japan Heart Foundation, The Mochida Memorial Foundation, and the German Genome Research Network.

References

1. Levy D, Garrison RJ, Savage DD, Kannel WB, Castelli WP. Prognostic implications of echocardiographically determined left ventricular mass in the Framingham Heart Study. *N Engl J Med*. 1990;322:1561–1566.
2. Morgan HE, Baker KM. Cardiac hypertrophy: mechanical, neuronal, and endocrine dependence. *Circulation*. 1991;83:13–25.
3. Molkentin JD, Dorn GW. Cytoplasmic signaling pathways that regulate cardiac hypertrophy. *Annu Rev Physiol*. 2001;63:391–426.
4. Sugden PH, Clerk A. Cellular mechanisms of cardiac hypertrophy. *J Mol Med*. 1998;76:725–746.
5. Newton AC. Regulation of protein kinase C. *Curr Opin Cell Biol*. 1997; 9:161–167.
6. Allo SN, Carl LL, Morgan HE. Acceleration of growth of cultured cardiomyocytes and translocation of protein kinase C. *Am J Physiol*. 1992;263:C319–C325.
7. Takeishi Y, Chu G, Kirkpatrick DL, Wakasaki H, Li Z, Kranias EG, King GL, Walsh RA. In vivo phosphorylation of cardiac troponin I by PKCβ2 decreases cardiomyocyte calcium responsiveness and contractility in transgenic mouse heart. *J Clin Invest*. 1998;102:72–78.
8. Bowling N, Walsh RA, Song G, Estridge T, Sandusky GE, Fouts RL, Mintze K, Pickard T, Roden R, Bristow MR, Sabbah HN, Mizrahi JL, Gromo G, King GL, Vlahos CJ. Increased protein kinase C activity and expression of Ca^{2+}-sensitive isoforms in the failing human heart. *Circulation*. 1999;99:384–391.
9. Takeishi Y, Bhagwat A, Ball NA, Kirkpatrick DL, Periasamy M, Walsh RA. Effect of angiotensin-converting enzyme inhibition on protein kinase C and SR proteins in heart failure. *Am J Physiol*. 1999;276:H53–H62.
10. Takeishi Y, Jalili T, Ball NA, Walsh RA. Responses of cardiac protein kinase C isoforms to distinct pathological stimuli are differentially regulated. *Circ Res*. 1999;85:264–271.
11. Takeishi Y, Ping P, Bolli R, Kirkpatrick DL, Hoit BD, Walsh RA. Transgenic overexpression of constitutively active protein kinase C ε causes concentric cardiac hypertrophy. *Circ Res*. 2000;86:1218–1223.
12. Sakane F, Yamada K, Kanoh H, Yokoyama C, Tanabe T. Porcine diacylglycerol kinase sequence has zinc finger and E-F hand motifs. *Nature*. 1990;344:345–348.
13. Topham MK, Prescott SM. Mammalian diacylglycerol kinases, a family of lipid kinases with signaling functions. *J Biol Chem*. 1999;274: 11447–11450.
14. Goto K, Kondo H. Diacylglycerol kinase in the central nervous system: molecular heterogeneity and gene expression. *Chem Phys Lipids*. 1999; 98:109–117.

15. Takeda M, Kagaya Y, Takahashi J, Sugie T, Ohta J, Watanabe J, Shirato K, Kondo H, Goto K. Gene expression and in situ localization of diacylglycerol kinase isozymes in normal and infarcted rat hearts: effects of captopril treatment. *Circ Res.* 2001;89:265–272.
16. Nitobe J, Yamaguchi S, Okuyama M, Nozaki N, Sata M, Miyamoto T, Takeishi Y, Kubota I, Tomoike H. Reactive oxygen species regulate FLICE inhibitory protein (FLIP) and susceptibility to Fas-mediated apoptosis in cardiac myocytes. *Cardiovasc Res.* 2003;57:119–128.
17. Strait JB, Martin JL, Bayer A, Mestril R, Eble DM, Samarel AM. Role of protein kinase C-epsilon in hypertrophy of cultured neonatal rat ventricular myocytes. *Am J Physiol Heart Circ Physiol.* 2001;280:H756–H766.
18. Yuki K, Suzuki T, Katoh S, Kakinuma Y, Miyauchi T, Mitsui Y. Endothelin-1 stimulates cardiomyocyte injury during mitochondrial dysfunction in culture. *Eur J Pharmacol.* 2001;431:163–170.
19. Goto K, Kondo H. A 104-kDa diacylglycerol kinase containing ankyrin-like repeats localizes in the cell nucleus. *Proc Natl Acad Sci U S A.* 1996;93:11196–11201.
20. Hozumi Y, Ito T, Nakano T, Nakagawa T, Aoyagi M, Kondo H, Goto K. Nuclear localization of diacylglycerol kinase ζ in neurons. *Eur J Neurosci.* 2003;18:1448–1457.
21. Seidler T, Miller S, Loughrey CM, Kania A, Burow A, Kettlewell S, Teucher N, Wagner S, Kogler H, Meyers MB, Hasenfuss G, Smith GL. Effects of adenovirus-mediated sorcin overexpression on excitation-contraction coupling in isolated rabbit cardiomyocytes. *Circ Res.* 2003;93:132–139.
22. Goetzl EJ, Lee H, Azuma T, Stossel TP, Turck CW, Karliner JS. Gelsolin binding and cellular presentation of lysophosphatidic acid. *J Biol Chem.* 2000;275:14573–14578.
23. Takeishi Y, Abe J, Lee JD, Kawakatsu H, Walsh RA, Berk BC. Differential regulation of p90 ribosomal S6 kinase and big mitogen-activated protein kinase 1 by ischemia/reperfusion and oxidative stress in perfused guinea pig hearts. *Circ Res.* 1999;85:1164–1172.
24. Takahashi H, Takeishi Y, Miyamoto T, Shishido T, Ariomoto T, Konta T, Miyashita T, Ito M, Kubota I. Protein kinase C and extracellular signal regulated kinase are involved in cardiac hypertrophy of rats with progressive renal injury. *Eur J Clin Invest.* 2004;34:85–93.
25. Miyashita T, Takeishi Y, Kubota I, Takahashi H, Kato S, Kubota I, Tomoike H. Calcineurin is involved in insulin-like growth factor-1-induced hypertrophy of cultured adult rat ventricular myocytes. *Jpn Circ J.* 2001;65:815–819.
26. Hirotani S, Otsu K, Nishida K, Higuchi Y, Morita T, Nakayama H, Yamaguchi O, Mano T, Matsumura Y, Ueno H, Tada M, Hori M. Involvement of nuclear factor-κB and apoptosis signal-regulating kinase 1 in G-protein-coupled receptor agonist-induced cardiomyocyte hypertrophy. *Circulation.* 2002;105:509–515.
27. Shishido T, Nozaki N, Yamaguchi S, Shibata Y, Nitobe J, Miyamoto T, Takahashi H, Arimoto T, Maeda K, Yamakawa M, Takeuchi O, Akira S, Takeishi Y, Kubota I. Toll-like receptor-2 modulates ventricular remodeling after myocardial infarction. *Circulation.* 2003;108:2905–2910.
28. Clerk A, Bogoyevitch MA, Andersson MB, Sugden PH. Differential activation of protein kinase C isoforms by endothelin-1 and phenylephrine and subsequent stimulation of p42 and p44 mitogen-activated protein kinases in ventricular myocytes cultured from neonatal rat hearts. *J Biol Chem.* 1994;269:32848–32857.
29. Fareh J, Touyz RM, Schiffrin EL, Thibault G. Endothelin-1 and angiotensin II receptors in cells from rat hypertrophied heart: receptor regulation and intracellular Ca^{2+} modulation. *Circ Res.* 1996;78:302–311.
30. Spieker LE, Noll G, Ruschitzka FT, Luscher TF. Endothelin receptor antagonists in congestive heart failure: a new therapeutic principle for the future? *J Am Coll Cardiol.* 2001;37:1493–1505.
31. Dhalla NS, Xu YJ, Sheu SS, Tappia PS, Panagia V. Phosphatidic acid: a potential signal transducer for cardiac hypertrophy. *J Mol Cell Cardiol.* 1997;29:2865–2871.
32. Exton JH. Phospholipase D: enzymology, mechanisms of regulation, and function. *Physiol Rev.* 1997;77:303–320.
33. Sugden PH. An overview of endothelin signaling in the cardiac myocyte. *J Mol Cell Cardiol.* 2003;35:871–886.
34. Yano M, Kim S, Izumi Y, Yamanaka S, Iwao H. Differential activation of cardiac c-jun amino-terminal kinase and extracellular signal-regulated kinase in angiotensin II-mediated hypertension. *Circ Res.* 1998;83:752–760.
35. Karin M. The regulation of AP-1 activity by mitogen-activated protein kinases. *J Biol Chem.* 1995;270:16483–16486.
36. Luo B, Prescott SM, Topham MK. Protein kinase C alpha phosphorylates and negatively regulates diacylglycerol kinase zeta. *J Biol Chem.* 2003;278:39542–39547.
37. Zhong XP, Hainey EA, Olenchock BA, Zhao H, Topham MK, Koretzky GA. Regulation of T cell receptor-induced activation of the Ras-ERK pathway by diacylglycerol kinase zeta. *J Biol Chem.* 2002;277:31089–31098.
38. Luo B, Prescott SM, Topham MK. Association of diacylglycerol kinase zeta with protein kinase C alpha: spatial regulation of diacylglycerol signaling. *J Cell Biol.* 2003;160:929–937.
39. Verrier E, Wang L, Wadham C, Albanese N, Hahn C, Gamble JR, Chatterjee VK, Vadas MA, Xia P. PPARγ agonists ameliorate endothelial cell activation via inhibition of diacylglycerol-protein kinase C signaling pathway: role of diacylglycerol kinase. *Circ Res.* 2004;94:1515–1522.

Circ J 2005; **69:** 277–282

Clinical Characteristics of Heart Disease Patients With a Good Prognosis in Spite of Markedly Increased Plasma Levels of Type-B Natriuretic Peptide (BNP)

—— Anomalous Behavior of Plasma BNP in Hypertrophic Cardiomyopathy ——

Ichiro Takeuchi, MD; Takayuki Inomata, MD; Mototsugu Nishii, MD; Toshimi Koitabashi, MD; Hironari Nakano, MD; Hisahito Shinagawa, MD; Hitoshi Takehana, MD; Tohru Izumi, MD

Background Although it is not rare to encounter patients with plasma B-type natriuretic peptide (BNP) levels unequivalent to the severity of heart failure (HF), there has been little investigation to clarify the causative background of this phenomenon.

Methods and Results Among the 1,838 outpatients whose plasma BNP was measured, persistently increased levels of BNP above 500 pg/ml was observed for more than 6 months in 14 subjects with few HF symptoms. Among these, all of 4 patients without any following cardiac events (E–/high) for 12 months showed hypertrophic nonobstructive cardiomyopathy (HNCM). When we compared the clinical parameters of these patients with those of 22 HNCM patients without any following cardiac events whose plasma BNP levels were less than 200 pg/ml, there were only 2 clinical characteristics to be distinguished: (i) plasma renin activity (PRA) and norepinephrine (NE) levels were low in spite of markedly increased levels of plasma BNP in E–/high HNCM; and (ii) echocardiographic investigation revealed that only global left atrial fractional shortening was significantly lower in E–/high HNCM.

Conclusions Plasma BNP levels do not always reflect the severity of HF in HNCM. It might be considered to utilize other clinical parameters such as NE and PRA to recognize HF severity in such patients. (*Circ J* 2005; **69:** 277–282)

Key Words: Heart failure; Hypertrophic cardiomyopathies; Natriuretic peptides; Prognosis

Type-B natriuretic peptide (BNP) is a predominantly ventricle-derived, cardiac neurohormone that promotes natriuresis and reduces vascular tone in an endocrine fashion to relieve heart failure (HF) status[1]. As plasma levels of BNP are associated well with the severity[2] and prognosis[3,4] of HF, BNP is now widely used as a useful clinical marker for differential diagnosis[5–7] and adequate management[8,9] for HF. It is not rare, however, to encounter patients with plasma BNP levels unequivalent to the severity of HF. This finding might suggest that BNP levels should be individually evaluated according to the patients' background including basal cardiac diseases.

In the present study, we focused on the profiles of clinically-stable outpatients with markedly increased plasma BNP levels in spite of few HF symptoms, especially those with hypertrophic cardiomyopathy (HCM). The causative mechanism of the discrepancy between HF severity and plasma BNP levels is discussed.

(Received October 18, 2004; revised manuscript received December 8, 2004; accepted December 24, 2004)

Department of Internal Medicine & Cardiology, Kitasato University School of Medicine, Sagamihara, Japan

Grants provided from Ishidu Shun Memorial Scholarship, the Postgraduate Research Project at Kitasato University, Kitasato University Research Grant for Young Researchers, and the Parents' Association Grant of Kitasato University School of Medicine.

Mailing address: Ichiro Takeuchi, MD, Department of Internal Medicine & Cardiology, Kitasato University School of Medicine, 1-15-1 Kitasato, Sagamihara 228-8555, Japan. E-mail: takeuchi@aqr.calmnet.ne.jp

Methods

Study Patients

The study population consisted of a consecutive series of 1,838 outpatients whose plasma concentration of BNP was measured at Kitasato University Hospital from January 2001 to July 2002. Among these, 42 patients who were admitted because of HF exacerbation soon after the BNP measurement and 7 patients with end-stage renal failure with hemodialysis were excluded from the analyses.

Clinical Measurement of HF

At the outpatient visit on the first measurement of plasma BNP, functional capacity according to the New York Heart Association (NYHA) was classified and clinical status including physical exams, blood tests, chest X-rays and ultrasound echocardiograms (UCG) were undertaken. Survival and cardiac events of HF exacerbation recognized by medical intensification or hospital admission were assessed at 12-month follow-up from the first measurement of plasma BNP.

Table 1 Comparison of Basal Characteristics Between Stable Outpatients Whose Plasma Type-B Natriuretic Peptide (BNP) was Markedly Increased With and Without Following Cardiac Events

	E+/high	*E−/high*	
n	*10*	*4*	
Age	*67±10*	*68±18*	*NS*
Men:women	*8:7*	*1:3*	*NS*
NYHA			
I	*8*	*4*	*NS*
II	*2*	*0*	
III	*0*	*0*	
IV	*0*	*0*	
Basal heart disease			
HCM	*0*	*4*	
DCM	*3*	*0*	
IHD	*7*	*0*	
LVDd (mm)	*5.4±0.4*	*5.0±0.3*	*NS*
LVEF (%)	*35.8±9.8*	*64.7±3.6*	*<0.01*
(IVSt+PWt)/2 (mm)	*9.4±1.9*	*15±2.0*	*<0.01*
BNP (pg/ml)	*596±117*	*565±51*	*NS*
Hb (g/dl)	*11.3±3.9*	*13.9±0.6*	*NS*
Cre (mg/dl)	*1.1±0.2*	*1.0±0.1*	*NS*

E+/high, patients with persistently increased levels of plasma BNP above 500pg/ml for more than 6 months who had cardiac events during the 12 months follow up period; E−/high, patients with persistently increased levels of plasma BNP above 500pg/ml for more than 6 months who had no cardiac events during the same follow up period; NYHA, New York Heart Association; HCM, hypertrophic cardiomyopathy; DCM, dilated cardiomyopathy; IHD, ischemic heart disease; LVDd, left ventricular end-diastolic dimension; LVEF, left ventricular ejection fraction; IVSt, wall thickness of interventricular septum; PWt, left ventricular posterior wall thickness; Hb, hemoglobin; Cre, serum creatinine; NS, not significant.

Venous blood samples for neurohumoral factors were taken from an antecubital vein after 15 min of rest. Plasma BNP and type-A natriuretic peptide (ANP) were determined by immunoradiometric assay (Shionoria BNP/ANP®). Plasma renin activity (PRA) was measured using the radioimmunoassay (RIA) double-antibody method, and the plasma aldosterone concentration (PAC) was measured using the RIA solid-phase method. Plasma norepinephrine (NE) was determined by high-performance liquid chromatography.

Pulmonary capillary wedge pressure (PCWP) was estimated by 2 blind observers using radiographic pulmonary vasculature and alveolar/interstitial edema as Turner has reported[10] Briefly, presumed PCWP was calculated using 5-grade estimation according to the pulmonary capillary redistribution compared with the upper and lower lung, and interstitial edema of chest X-rays at the upright position. The inter- and intra-observer variance was less than 5%.

M-mode images of UCG were obtained in left parasternal long-axis views using a SONOS 500 (Hewlett Packard, USA) to measure chamber dimensions and wall thicknesses. Global left atrium fractional shortening (gLAFS: 100 [(LAd_{max}−LAd_{min})/LAd_{max}]) (LAd_{max}, maximum left atrial (LA) diameter at the ventricular end-systole; LAd_{min}, minimum LA diameter at the end of atrial contraction)[11] and left ventricular (LV) mass (LVM: 1.04 [(IVSt+LVDd+PWt)^3−LVDd^3]−13.6) (IVSt, wall thickness of intraventricular septum; LVDd, LV end-diastolic dimension; PWt, LV posterior wall thickness)[12] were calculated as previously reported. The LV ejection fraction (LVEF) was derived from 2-dimentional apical 4-chamber views with a modified Simpson's rule argorithm[13] The transmitral pulsed Doppler velocity recordings were used to derive measurements as follows: E and A velocities were the peak values reached in early diastole and after atrial contraction, respectively, and deceleration time was the interval from the E-wave peak to the decline of the velocity to baseline. The peak instantaneous LV outflow tract (LVOT) gradient was estimated under basal conditions with continuous-wave Doppler and the patients with hypertrophic cardiomyopathy (HCM) with a LVOT gradient >30 mmHg were classified as having hypertrophic obstructive cardiomyopathy (HOCM). The diagnosis of HCM was made according to the definition and classification proposed by the World Health Organization/International Society and Federation of Cardiology Task Force![14]

Soon after UCG analysis, thalium-201 (^{201}Tl) myocardial scintigraphy was performed by peak exercise using a multistage bicycle ergometer or intravenous infusion of dipyridamole (0.57 mg/kg) in HCM patients. Stress-induced myocardial ischemia was defined as the presence of a reversible regional perfusion abnormality at the late phase redistribution in the images of single-photon emission computed tomography (SPECT). In patients without specific electrocardiographic findings for LV hypertrophy including ST-T strain pattern who rejected the scintigraphy, more than 0.2 mV of ST-segment depression at peak exercise during the treadmill exercise stress test was considered to be positive for myocardial ischemia.

All the study subjects signed informed consent forms before the study, and the study protocol was approved by the research council of our institution.

Statistical Analysis

Statistical analyses were performed by the Mann−Whitney U-test. Data are expressed as mean±SD. Statistical significance was defined as $p<0.05$.

Results

Persistently increased levels of plasma BNP above 500 pg/ml were observed for more than 6 months in 14 (0.78%, out of 1,789) outpatients. There were no lethal events in these patients during a 12-month follow-up. However, 10 patients (7 with ischemic heart disease and 3 with dilated cardiomyopathy) had cardiac events with HF

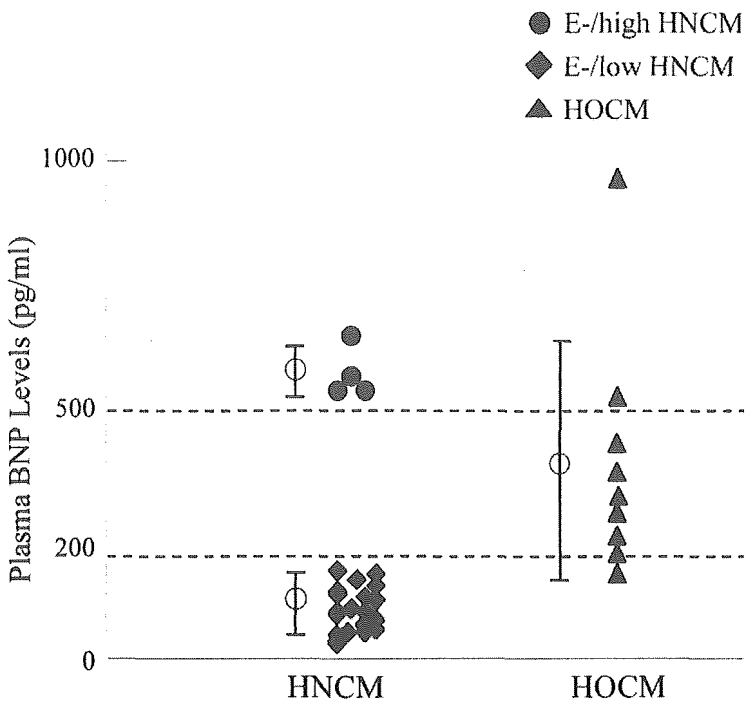

Fig 1. Comparison of plasma type-B natriuretic peptide (BNP) levels among patients with hypertrophic cardiomyopathy (HCM). The plasma BNP was higher in E–/high nonobstructive hypertrophic cardiomyopathy (HNCM) than not only that in E–/low HNCM but also most of hypertrophic obstructive cardiomyopathy (HOCM).
E–/high, event-free HNCM patients with persistently increased levels of plasma BNP above 500 pg/ml for more than 6 months; E–/low, event-free HNCM patients with plasma BNP less than 200 pg/ml.

Table 2 Comparison of Patients' Characteristics Including Ultrasound Echocardiograms (UCG) Findings and Neurohumoral Factors Between Event-Free Hypertrophic Nonobstructive Cardiomyopathy (HNCM) With High and Low Levels of Plasma BNP

	E–/high HNCM	*E–/low HNCM*	
n	4	22	
Age	68±18	58±12	*NS*
Men:women	1:3	15:7	*NS*
NYHA			
I	4	21	*NS*
II	0	1	
III	0	0	
Af	1	1	*NS*
HR (/min)	62±7	65±5	*NS*
sBP (mmHg)	116±12	129±10	*NS*
Hb (g/dl)	13.9±0.6	14.5±2.9	*NS*
Cre (mg/dl)	1.0±0.1	1.0±0.1	*NS*
p-PCWP (mmHg)	11±3	10±1	*NS*
Positive for MI	0	2	*NS*
UCG findings			
LVEF (%)	64.7±3.6	61.6±3.6	*NS*
IVSt (mm)	18.5±3.1	17.3±1.9	*NS*
PWt (mm)	11.2±2.0	11.4±1.5	*NS*
IVSt/PWt (mm)	1.5±0.3	1.5±0.2	*NS*
LAd (mm)	44.5±4.6	45.5±8.4	*NS*
DCT (ms)	218±59	239±43	*NS*
E/A	0.97±0.7	0.95±0.45	*NS*
gLFAS (%)	10.3±3.0	17.9±5.4	*<0.05*
LVOT-PG (mmHg)	6.6±5.2	8.2±8.1	*NS*
LVMI (g/m²)	270±53	223±34	*NS*
Neurohumoral factors			
BNP (pg/ml)	565±51	108±63	*<0.01*
ANP (pg/ml)	173±70	57±40	*<0.01*
PRA (ng/ml/h)	0.6±0.5	1.8±1.2	*<0.05*
PAC (pg/ml)	52±26	79±47	*NS*
NE (pg/ml)	498±232	704±321	*NS*
BNP/NE	1.3±0.5	0.3±0.2	*<0.01*

E–/high, event-free HNCM patients with persistently increased levels of plasma BNP above 500 pg/ml for more than 6 months; E–/low, event-free HNCM patients with plasma BNP less than 200 pg/ml; Af, atrial fibrillation; HR, heart rate; sBP, systolic blood pressure; p-PCWP, pulmonary capillary wedge pressure presumed by radiographic pulmonary vasculature; MI, myocardial ischemia; LAd, left atrium dimension; DCT, deceleration time; E/A, the ratio of E wave to A wave; gLFAS, global left atrium fraction shortening; LVOT-PG, left ventricular outflow pressure gradient; LVMI, left ventricular mass index; ANP, type-A natriuretic peptide; PRA, plasma renin activity; PAC, plasma concentration of aldosterone; NE, plasma norepinephrine.

exacerbation (E+/high) during an observational period, while all 4 patients without any following cardiac events (E−/high) had hypertrophic nonobstructive cardiomyopathy (HNCM) as basal heart diseases (Table 1).

To investigate the clinical characteristics and causative mechanisms of paradoxical phenomenon as E−/high, we compared the clinical parameters of these 4 E−/high HNCM patients with those of another 22 consecutive clinically-stable HNCM patients without following cardiac events whose plasma BNP levels were less than 200 pg/ml (E−/low), as well as 9 HOCM patients. The plasma BNP was higher in E−/high HNCM (565±51 pg/ml), not only in E−/low HNCM (108±63 pg/ml), but also in most of HOCM (387±238 pg/ml) (Fig 1). Among estimated clinical parameters for neurohumoral factors, PRA, PAC and NE was low in spite of markedly increased levels of plasma BNP in E−/high HNCM. The significant difference of the ratio of BNP to NE between the 2 groups of HNCM demonstrated the discrepancy between plasma BNP and NE, a representative biomarker for HF severity[15] other than BNP, in E−/high HNCM (Table 2). However, the UCG study demonstrated that there was no significant difference of LV diastolic properties implied from transmitral Doppler flow, LVM and LVOT pressure gradients between E−/high and E−/low HNCM. gLFAS was the only echocardiographic parameter to significantly differentiate these 2 groups. There was no significant difference of positive myocardial ischemia between E−/high HNCM (n=0) and E−/low HNCM (n=2) (Table 2).

Discussion

The plasma level of BNP is determined under the balance sheet between myocardial production and peripheral clearance of BNP. In addition to the secretion from the kidney, enzymatic and receptor clearance pathways contribute to natriuretic peptide clearance through neutral endopeptidase and the guanylyl cyclase (GC)-A and GC-C receptors, respectively.[16] It has been reported that renal dysfunction, age, anemia, or gender could influence these clearance pathways to cause elevation of plasma BNP levels.[17–20] We could not, however, find any significant difference of such clinical parameters as to affect BNP clearance between E−/high and E−/low HNCM (Table 2).

However, BNP release appeared to be directly proportional to ventricular volume expansion and pressure overload.[21] Nevertheless, there were no significant differences of hemodynamic status which could influence ventricular wall stress such as systemic blood pressure or the degree of LVOT obstruction between the 2 HNCM groups (Table 2). As clinically stable outpatients with few HF signs were focused on in the current study, we had to utilize noninvasive clinical parameters to imply LV overload. Doppler-derived transmitral velocity profiles are routinely used to evaluate LV diastolic properties together with LV filling pressure.[22] However, this is not the case with HCM; gLAFS from the M-mode echocardiographic profiles of the left atrium, not mitral Doppler indexes, has a reverse correlation with left ventricular end-diastolic pressure (LVEDP).[11] Although the significantly lower gLAFS could suggest that elevated LVEDP might be one of the causes of increased BNP in the E−/high HNCM. However, pulmonary venous pressure presumed from pulmonary vasculature in chest X-rays according to Turner's calculation[10] was not elevated in this group. Why did the E−/high HNCM patients have few signs of pulmonary congestion in spite of elevated LVEDP? Braunwald and Frahm reported the relationship between mean LA pressure (MLAP) and LVEDP using direct intracardiac pressure measurement.[23] Unlike the subjects with normal cardiovascular systems, the LVEDP exceeded MLAP by 9 mmHg on average in patients with left ventricular hypertrophy, especially with concomitant elevated LVEDP. Although the specific mechanism was not clarified, the volume of blood contributed by atrial systole might be greater than normal in the patients with LVH as the thickened LV wall presumably results in diminished compliance. Hence the dissociation between LVEDP and LA internal pressure in determining the symptoms of left heart failure could be the causative mechanism of the clinically stable status without pulmonary congestion in spite of elevated LVEDP in E−/high HNCM.

Another point of view to explain the mechanism of increasing BNP production is the pathophysiology of myocardial hypertrophy in HCM. It is known that natriuretic peptides are overexpressed in hypertrophied myocardium as a result of retranscription of embryonic cardiac-specific genes.[24] Although it is certain that the plasma BNP levels are increased in hypertensive patients with left ventricular hypertrophy leading to LV diastolic dysfunction,[25] the mean value of plasma BNP in such patients appears to be approximately 40 pg/ml, as reported in Japanese subjects.[26] This means that the mechanism of the markedly increased levels of plasma BNP in some cases with HCM might differ from that in hypertensive heart disease. Hasegawa et al[27] speculated that increased levels of plasma BNP disproportional to LVEDP or LVM[28,29] in HOCM could be contributed to morphological changes such as interstitial fibrosis and myocardial disarray. In the present study histological assessment by cardiac biopsy was not performed because the study patients were clinically stable outpatients. Genetic analyses have shown causal mutation of genes encoding cardiac sarcomere proteins,[30] suggesting impaired force production[31–33] associated with the inefficient use of adenosine triphosphate (ATP) as the crucial disease mechanism.[32] Therefore, hypertrophy could possibly be a means of compensation for low force generation although precise pathomechanisms have not yet been clarified.[34] Elucidating the causative mechanisms for myocardial hypertrophy could lead to understanding of the setting of plasma BNP levels through myocardial BNP production in HCM. Moreover, it has been reported that concomitant myocardial ischemia could induce the elevated plasma BNP in HCM;[35] myocardial ischemia was not evidently observed in E−/high HNCM.

Various circulating neurohumoral factors that increase in patients with HF are thought to play important roles in the pathogenesis of HF. Neurohumoral systems including the renin-angiotensin-aldosterone system (RAAS), sympathetic nervous system, vasopressin, endothelin, and natriuretic peptides cooperatively modulate both vascular tone and the retention of salt and water.[2] The natriuretic peptide family including BNP plays important roles to diminish neurohumoral activation for HF exacerbation.[2,5] Inversely, neurohumoral activation, namely from RAAS and the sympathetic nervous system, induces the release and secretion of natriuretic peptides.[36] This means that the activity of accelerating factors such as NE and protective factors such as BNP should be simultaneously altered in HF.[37] We could notice in the current study, however, that plasma PRA and NE were disproportionally low to the markedly increased

levels of plasma BNP in E–/high HNCM. This could be derived from the different form of secretion into the systemic bloodstream. Circulatory NE in blood is secreted from sympathetic nerve terminals and the majority of which are located in peripheral vessels, some in the adrenal medulla, and only a few in the myocardium.[38] The major site of release of circulating renin is the juxtaglomerular apparatus of the kidney, where multiple stimuli may contribute to renal release of renin into the systemic circulation, including increased renal sympathetic efferent activity, decreased distal tubular sodium delivery, and reduced renal perfusion pressure.[39] That is to say, the majority of circulatory NE and renin is derived from the secretion from systemic organs other than the heart in situ. In patients with E–/high HNCM, the increased levels of plasma BNP might reflect myocardial hypertrophy peculiar to HCM, not the severity of HF implicated by ventricular overloading. Plasma NE levels or PRA, however, might rather reflect the general status or severity of HF adequately in such patients. That is, disproportion between BNP and PRA/NE may often be observed in compensated patients with HNCM.

Study Limitations

We attempted to compare the clinical values between E–/high and E–/low HNCM to draw the causative pathomechanism to increase BNP independently from the clinical HF status. It is certain that some limitations of the study must be acknowledged because there was insufficient statistical power in some analyses owing to only 4 E–/high HNCM to be compared. Despite these limitations, however, it was noteworthy that 4 patients whose level was over 500 pg/ml without following cardiac events abstracted from a large number of outpatients all showed HNCM as basal heart diseases. In other words, the increase in BNP concentration up to several hundred pg/ml does not often indicate the prognosis of HNCM patients. Further prospective studies addressing the pathogenesis of increasing BNP in HNCM in conjunction with the cardiac events seem warranted.

Acknowledgements

The present study was supported in part by a grant-in-aid for scientific research from Ishidu Shun Memorial Scholarship, the Postgraduate Research Project at Kitasato University, Kitasato University Research Grant for Young Researchers, and the Parents' Association Grant of Kitasato University School of Medicine.

References

1. Mukoyama M, Nakao K, Hosoda K, Suga S, Saito Y, Ogawa Y, et al. Brain natriuretic peptide as a novel cardiac hormone in humans. Evidence for an exquisite dual natriuretic peptide system, atrial natriuretic peptide and brain natriuretic peptide. *J Clin Invest* 1991; **87:** 1402–1412.
2. Tsutamoto T, Wada A, Maeda K, Hisanaga T, Maeda Y, Fukai D, et al. Attenuation of compensation of endogenous cardiac natriuretic peptide system in chronic heart failure: Prognostic role of plasma brain natriuretic peptide concentration in patients with chronic symptomatic left ventricular dysfunction. *Circulation* 1997; **96:** 509–516.
3. Berger R, Huelsman M, Strecker K, Bojic A, Maser P, Stanek B, et al. B-type natriuretic peptide predicts sudden death in patients with chronic heart failure. *Circulation* 2002; **105:** 2392–2397.
4. Koseki Y, Watanabe J, Shinozaki T, Sakuma M, Komaru T, Fukuchi M, et al. Characteristics and 1-year prognosis of medically treated patients with chronic heart failure in Japan–chronic heart failure analysis registry in Tohoku district (CHART). *Circ J* 2003; **67:** 431–436.
5. McCullough PA, Nowak RM, McCord J, Hollander JE, Herrmann HC, Steg PG, et al. B-type natriuretic peptide and clinical judgement in emergency diagnosis of heart failure: Analysis from Breathing Not Properly (BNP) Multinational Study. *Circulation* 2002; **106:** 416–422.
6. Morrison LK, Harrison A, Krishnaswamy P, Kazanegra R, Clopton P, Maisel A. Utility of rapid B-natriuretic peptide assay in differentiating congestive heart failure from lung disease in patients presenting with dyspnea. *J Am Coll Cardiol* 2002; **39:** 202–209.
7. Nagao K, Hayashi N, Kanmatsuse K, Kikuchi S, Kikushima K, Watanabe K, et al. B-type natriuretic peptide as a marker of resuscitation in patients with cardiac arrest outside the hospital. *Circ J* 2004; **68:** 477–482.
8. Troughton RW, Frampton CM, Yandle TG, Espiner EA, Nicholls MG, Richards AM. Treatment of heart failure guided by plasma amino-terminal brain natriuretic peptide (N-BNP) concentrations. *Lancet* 2000; **355:** 1126–1139.
9. Inomata T, Nishii M, Takehana H, Takeuchi I, Koitabashi T, Nakano H, et al. Brain natriuretic peptide-guided treatment reduces cardiovascular events of heart failure in outpatient management (abstract). *Circulation* 2002; **106:** 416.
10. Turner AF. The chest radiograph: A systematic approach to interpretation for the internist. *Curr Probl Cardiol* 1978; **3:** 1–50.
11. Briguori C, Betocchi S, Losi MA, Manganelli F, Pace L, Boccalatte M, et al. Noninvasive evaluation of left ventricular diastolic function in hypertrophic cardiomyopathy. *Am J Cardiol* 1998; **81:** 180–187.
12. Devereux RB, Alonso DR, Lutas EM, Gottlieb GJ, Campo E, Sachs I, et al. Echocardiographic assessment of left ventricular hypertrophy: Comparison to necropsy findings. *Am J Cardiol* 1986; **57:** 450–458.
13. Schiller NB, Acquatella H, Ports TA, Drew D, Goerke J, Ringertz H, et al. Left ventricular volume from paired biplane two-dimensional echocardiography. *Circulation* 1979; **60:** 547–555.
14. WHO/ISFC Task Force. Report of the WHO/ISFC Task Force on the Definition and Classification of Cardiomyopathies. *Br Heart J* 1980; **44:** 672–673.
15. Cohn JN, Levine TB, Olivari MT, Garberg V, Lura D, Francis GS, et al. Plasma norepinephrine as a guide to prognosis in patients with chronic congestive heart failure. *N Engl J Med* 1984; **311:** 819–823.
16. Charles CJ, Espiner EA, Nicholls MG, Richards AM, Yandle TG, Protter A, et al. Clearance receptors and endopeptidase: Equal role in natriuretic peptide metabolism in conscious sheep. *Am J Physiol* 1996; **271:** 373–380.
17. Nomura H, Hayashi T, Esaki T, Kanda S, Kano H, Hattori A, et al. Standardization of plasma brain natriuretic peptide concentrations in older Japanese-relationship to latent renal dysfunction and ischemic heart disease. *J Am Geriatr Soc* 2002; **50:** 1504–1509.
18. McCullough PA, Duc P, Omland T, McCord J, Nowak RM, Hollander JE, et al. B-type natriuretic peptide and renal function in the diagnosis of heart failure: An analysis from the Breathing Not Properly Multinational Study. *Am J Kidney Dis* 2003; **41:** 571–579.
19. Redfield MM, Rodehefer RJ, Jacobsen SJ, Mahoney DW, Bailey KR, Burnett JC. Plasma brain natriuretic peptide concentration: Impact of age and gender. *J Am Coll Cardiol* 2002; **40:** 976–982.
20. Kikuchi M, Inagaki T. Atrial natriuretic peptide in aged patients with iron deficiency anemia. *Arch Gerontol Geriatr* 1999; **28:** 105–115.
21. Maeda K, Tsutamoto T, Wada A, Hisanaga T, Kinoshita M. Plasma brain natriuretic peptide as a biochemical marker of high left ventricular end-diastolic pressure in patients with symptomatic left ventricular dysfunction. *Am Heart J* 1998; **135:** 825–832.
22. Ishida Y, Meisner JS, Tsujioka K, Gallo JI, Yoran C, Frater RW, et al. Left ventricular filling dynamics: Influence of left ventricular relaxation and left atrial pressure. *Circulation* 1986; **74:** 187–196.
23. Braunwald E, Frahm CJ. Studies on Starling's law of the heart, IV: Observations on the hemodynamic functions of the left atrium in man. *Circulation* 1961; **24:** 633–642.
24. Bruneau BG. Transcriptional regulation of vertebrate cardiac morphogenesis. *Circ Res* 2002; **90:** 509–519.
25. Ogino K, Ogura K, Kinugawa T, Osaki S, Kato M, Furuse Y, et al. Neurohumoral profiles in patients with hypertrophic cardiomyopathy-differences to hypertensive left ventricular hypertrophy. *Circ J* 2004; **68:** 444–450.
26. Kohno M, Horio T, Yokokawa K, Murakawa K, Yasunari K, Akioka K, et al. Brain natriuretic peptide as a cardiac hormone in essential hypertension. *Am J Med* 1992; **92:** 29–34.
27. Hasegawa K, Fujiwara H, Doyama K, Miyatake M, Fujiwara T, Suga S, et al. Ventricular expression of brain natriuretic peptide in hypertrophic cardiomyopathy. *Circulation* 1993; **88:** 372–380.
28. Nishigaki K, Tomita M, Kagawa K, Noda T, Minatoguchi S, Oda H, et al. Marked expression of plasma brain natriuretic peptide is a special feature of hypertrophic obstructive cardiomyopathy. *J Am Coll Cardiol* 1996; **28:** 1234–1242.
29. Briguori C, Betocchi S, Manganelli F, Gigante B, Losi MA, Ciampi Q, et al. Determinants and clinical significance of natriuretic peptides

and hypertrophic cardiomyopathy. *Eur Heart J* 2001; **22:** 1328–1336.
30. Franz WM, Muller OJ, Katus HA. Cardiomyopathies: From genetics to the prospect of treatment. *Lancet* 2001; **358:** 1627–1637.
31. Lankford EB, Epstein ND, Fananapazir L, Sweeney HL. Abnormal contractile properties of muscle fibers expressing beta-myosin heavy chain gene mutations in patients with hypertrophic cardiomyopathy. *J Clin Invest* 1995; **95:** 1409–1415.
32. Elliott K, Watkins H, Redwood CS. Altered regulatory properties of human cardiac troponin I mutants that cause hypertrophic cardiomyopathy. *J Biol Chem* 2000; **275:** 22069–22074.
33. Sanbe A, Nelson D, Gulick J, Setser E, Osinska H, Wang X, et al. In vivo analysis of an essential myosin light chain mutation linked to familial hypertrophic cardiomyopathy. *Circ Res* 2000; **87:** 296–302.
34. Paulus WJ. Natriuretic peptides to probe haemodynamic overload in hypertrophic cardiomyopathy. *Eur Heart J* 2001; **22:** 1249–1251.
35. Nakamura T, Sakamoto K, Yamano T, Kikkawa M, Zen K, Hikosaka T, et al. Increased plasma brain natriuretic peptide level as a guide for silent myocardial ischemia in patients with non-obstructive hypertrophic cardiomyopathy. *J Am Coll Cardiol* 2002; **39:** 1657–1663.
36. Yoshimura M, Yasue H, Morita E, Sakaino N, Jougasaki M, Kurose M, et al. Hemodynamic, renal, and hormonal responses to brain natriuretic peptide infusion in patients with congestive heart failure. *Circulation* 1991; **84:** 1581–1588.
37. Latini R, Masson S, Anand I, Salio M, Hester A, Judd D, et al. The comparative prognostic value of plasma neurohormones at baseline in patients with heart failure enrolled in Val-HeFT. *Eur Heart J* 2004; **25:** 292–299.
38. Francis GS, Benedict C, Johnston DE, Kirlin PC, Nkeklas J, Liang CS, et al. Comparison of neuroendocrine activation in patients with left ventricular dysfunction with and without congestive heart failure. A substudy of the Studies of Left Ventricular Dysfunction (SOLVD). *Circulation* 1990; **82:** 1724–1729.
39. Paganelli WC, Creager MA, Dzau VJ. Cardiac regulation of renal function. *In*: Cheng TO, editor. International Textbook of Cardiology. New York: Pergammon Press; 1986; 1010–1020.

Circulation Research
JOURNAL OF THE AMERICAN HEART ASSOCIATION

American Heart Association®
Learn and Live℠

Creation of a Genetic Calcium Channel Blocker by Targeted Gem Gene Transfer in the Heart

Mitsushige Murata, Eugenio Cingolani, Amy D. McDonald, J. Kevin Donahue and Eduardo Marbán

Circ. Res. 2004;95;398-405; originally published online Jul 8, 2004;
DOI: 10.1161/01.RES.0000138449.85324.c5
Circulation Research is published by the American Heart Association. 7272 Greenville Avenue, Dallas, TX 72514
 Print ISSN: 0009-7330. Online ISSN: 1524-4571